Master stability functions for complete, intralayer, and interlayer synchronization in multiplex networks of coupled Rössler oscillators

Longkun Tang, Xiaoqun Wu, Jinhu Lü, Jun-an Lu, and Raissa M. D'Souza

Phys. Rev. E **99**, 012304 — Published 3 January 2019

DOI: 10.1103/PhysRevE.99.012304

Master stability functions for complete, intra-layer and inter-layer synchronization in multiplex networks of coupled Rösslers

Longkun Tang,[1,*] Xiaoqun Wu,[2,3] Jinhu Lü,[4] Jun-an Lu,[2] and Raissa M. D'Souza[3]

[1]*Fujian Province University Key Laboratory of Computation Science, School of Mathematical Science, Huaqiao University, Quanzhou 362021, China.*

[2]*School of Mathematics and Statistics, Wuhan University, Wuhan 430072, China.*

[3]*Department of Computer Science, University of California, Davis CA 95616, USA.*

[4]*Institute of Systems Science, Academy of Mathematics and Systems Science, Chinese Academy of Sciences, Beijing 100190, China.*

Abstract

Synchronization phenomena are of broad interest across disciplines and increasingly of interest in a multiplex network setting. For the multiplex network of coupled Rössler oscillators, here we show how the Master Stability Function, a celebrated framework for analyzing synchronization on a single network, can be extended to certain classes of multiplex networks with different intra-layer and inter-layer coupling functions. We derive three master stability equations that determine respectively the necessary regions of complete synchronization, intra-layer synchronization and inter-layer synchronization. We calculate these three regions explicitly for the case of a two-layer network of Rössler oscillators and show that the overlap of the regions determines the type of synchronization achieved. In particular, if the inter- or intra-layer coupling function is such that the inter-layer or intra-layer synchronization region is empty, complete synchronization cannot be achieved regardless of the coupling strength. Furthermore, for any network structure, the occurrence of intra-layer and inter-layer synchronization depend mainly on the coupling functions of nodes within a layer and across layers, respectively. Our mathematical analysis requires that the intra- and inter-layer supra-Laplacians commute. But we show this is only a sufficient, and not necessary, condition and that the results can be applied more generally.

Keywords: Multiplex network; master stability function; complete synchronization; intra-layer synchronization; inter-layer synchronization; synchronized region.

* To whom correspondence should be addressed: tomlk@hqu.edu.cn

I. INTRODUCTION

Synchronization in a network of connected elements is essential to the proper functioning of a wide variety of natural and engineered systems, from brain networks to electric power grids. This has stimulated a large number of investigations into synchronization properties of complex networks, with small-world, scale-free and other types of topologies [1–15]. Yet many synchronization phenomena, as in electrical power grids, do not involve a single network in isolation but rely on the complete synchronization of a collection of smaller networks. And more generally, beyond single networks, we are now understanding that interactions between networks are increasingly important and that interactions can impact the dynamical processes [16–21]. One paradigm that captures many real-world interdependent networks is that of multiplex networks. Here the same set of nodes exist in multiple layers of networks, where each layer represents a different interaction type, the internal state of the corresponding nodes in each layer can be distinct, and the connectivity pattern between nodes in each layer can be distinct [22, 23]. As an example consider the online social system of a set of individuals. They may interact on Twitter or on Facebook or on Linked-in or on some combination of all three, and each layer can have its own connectivity pattern, yet there is typically influence propagated between them [24]. Given the need to study dynamical processes on layered complex networks, and the broad applicability of synchronization, here we study synchronization phenomena on multiplex networks, an area that has attracted increasing attention in the past few years.

One of the most important methods to study network synchronization on single networks is the master stability function (MSF) method proposed by Pecora and Carroll [25]. As established via the MSF approach, whether or not a network can achieve synchronization is determined not only by the network structure, but also by the nodal dynamics and by the inner coupling function which describes the interactions among the different components of the state vectors of connected nodes [26–28]. In other words, the nodal dynamics, the network topology and the inner coupling function are three basic elements in studying network synchronization. The latter two are paid most main attention, and the former is generally set as some specific chaotic system. Such as, Lorenz, Chen's, Chua circuit, and Rössler systems, and so on. Here Rössler chaotic system is selected as the network nodal dynamics due to the fact that the system can be implemented by circuits and applied to

secure communication. More importantly, we focus on the different inner coupling functions within and across layers in the multiplex network setting, as well as the different intra-layer topologies.

Current studies of synchronization phenomena in multiplex networks analyze a multiplex network as a single large composite network with the topology being described by a supra-Laplacian matrix. This requires that the inner coupling function is the same regardless of whether the nodes are linked by an intra-layer or inter-layer edge and the MSF framework can thus be directly applied. The eigenvalues of this supra-Laplacian are then used to analyze the stability of the state of complete synchronization in multiplex networks. For example, Solé-Ribalta et al. [29] investigated the spectral properties of the Laplacian of multiplex networks, and discussed the synchronizability via the eigenratio of the Laplacian matrix. Aguirre et al. [30] studied the impact of the connector node degree on the synchronizability of two star networks with one inter-layer link and showed that connecting the high-degree (low-degree) nodes of each network is the most (least) effective strategy to achieve synchronization. Xu et al. [31] investigated the synchronizability of two-layer networks for three specific coupling patterns, and determined that there exists an optimal value of the inter-layer coupling strength for maximizing complete synchronization in the two-layer networks they analyze. Li et al. [32] investigated the sychronizability of a duplex network composed of two star networks with two inter-layer links by giving an analytical expression containing the largest and the smallest nonzero eigenvalues of the Laplacian matrix, the link weight, as well as the network size.

In 2012, Sorrentino et al. [33, 34] considered an innovative "hypernetwork" model consisting of one set of N nodes that interact via multiple types of coupling functions. Note the contrast with a multiplex network, where a set of N nodes exists on each one of M distinct layers (for a total of $M \times N$ nodes), and each node can be in a different state in each layer. (See for instance, Fig. 1.) In the "hypernetwork" model there are only N nodes in total and each node can be in only one state at any given time. As such, the focus is on complete synchronization and three situations are found where the network topology is such that one can decouple the effects of interaction functions from the structure of the networks and apply the MSF approach [33, 34]. Extremely recently, del Genio et al. extended this analysis to a broader range of scenarios, again using an MSF approach [35], and show how the "hypernetwork" model of [33, 34] is equivalent to a network where nodes have many

different interaction types (or "layers" of interaction). Although these works consider that nodes can interact with one another via different coupling functions, they do not capture the richness of phenomena that can occur in multiplex networks such as intra-layer and inter-layer synchronization.

Only limited studies thus far have focused on intra-layer and inter-layer synchronization. For example, Gambuzza et. al [36] analyzed synchronization of a population of oscillators indirectly coupled through an inhomogeneous medium. The system is formalised in terms of a two-layer network, where the top layer is composed of disconnected oscillators, and the bottom layer consists of oscillators coupled according to a given topology, and each node in the top layer is connected to its counterpart in the bottom layer. By numerical simulations, they have shown the onset of intra-layer synchronization without inter-layer coherence, that is, a state in which the nodes of a layer are synchronized between them without being synchronized with those of the other layer. Shortly afterwards, Sevilla-Escoboza et. al [37] investigated the inter-layer synchronization in a duplex network of identical layers, and showed that there are instances where each node in a given layer can synchronize with its replica in the other layer irrespective of whether or not intra-layer synchronization occurs. These findings into specific systems provide useful foundations for elucidating a more fundamental approach to analyzing synchronization phenomena in multiplex networks. In fact, as we will show herein, master stability equations can be derived to systematically predict when intra- and inter-layer synchronization are simultaneously supported and when they are not simultaneously supported for certain classes of multiplex networks.

Based on the above motivations, here we develop a Master Stability Function method which captures an essential feature of multiplex networks, that the inter-layer coupling function can be distinct from the intra-layer coupling function. Thus, distinct from previous approaches, we can analyze different kinds of coherent behaviors, including complete synchronization, intra-layer synchronization and inter-layer synchronization in multiplex networks, however, we are restricted to certain classes of topologies. In particular, we derive the master stability equation for a multiplex network where the supra-Laplacian of intra-layer connections and that of inter-layer connections commute, as defined in detail below. We further derive two reduced forms of the master stability equation corresponding to only inter-layer or intra-layer interactions. We then show how three different necessary regions for synchronization can be calculated from the MSF of the three master stability

equations. Finally we show how to explicitly apply the multiplex MSF by analyzing a specific example of two-layer network of Rössler oscillators with identical intra-layer topological structures and one-to-one inter-layer connections. For broader applicability of this multiplex MSF approach, we further illustrate that the three master stability equations can still be used to predict the area of synchronization for some classes of multiplex networks with non-commutative supra-Laplacians.

II. A MASTER STABILITY FUNCTION FRAMEWORK FOR CLASSES OF MULTIPLEX NETWORKS

A. A multiplex network model

We consider a multiplex network consisting of M layers each consisting of N nodes. The state of the i-th node in the k-th layer is specified by $\boldsymbol{x}_i^{(k)} = (x_{i1}^{(k)}, x_{i2}^{(k)}, \cdots, x_{im}^{(k)})^\top$, an $m-$dimensional state vector. The evolution of the full multiplex system can be written as:

$$\dot{\boldsymbol{x}}_i{}^{(k)} = f(\boldsymbol{x}_i^{(k)}) - c\sum_{j=1}^{N} l_{ij}^{(k)} H(\boldsymbol{x}_j{}^{(k)}) - d\sum_{l=1}^{M} d_{kl}\Gamma(\boldsymbol{x}_i^{(l)}),\ i = 1, 2, \cdots, N;\ k = 1, 2, \cdots, M, \quad (1)$$

where $\dot{\boldsymbol{x}}_i{}^{(k)} = f(\boldsymbol{x}_i^{(k)})$ $(i = 1, 2, \cdots, N;\ k = 1, 2, \cdots, M)$ describes the isolated dynamics for the i-th node in the k-th layer, and $f(\cdot) : \mathbb{R}^m \to \mathbb{R}^m$ is a well-defined vector function, $H(\cdot) : \mathbb{R}^m \to \mathbb{R}^m$ and c are the inner coupling function and coupling strength for nodes within each layer, respectively, and $\Gamma(\cdot) : \mathbb{R}^m \to \mathbb{R}^m$ and d are the inner coupling function and coupling strength for nodes across layers, respectively. For simplicity and clarity, here we let $H(\boldsymbol{x}) = H\boldsymbol{x}$ and $\Gamma(\boldsymbol{x}) = \Gamma\boldsymbol{x}$, namely the coupling functions between nodes are linear (thus we can also call H and Γ inner coupling matrices). Furthermore, the inner coupling matrix for nodes within one layer, H, is identical for all layers and the inner coupling matrix for nodes across two layers, Γ, is the same for all pairs of layers.

Elements $l_{ij}^{(k)}$ describe the Laplacian matrix of nodes within the k-th layer. Explicitly, if the i-th node is connected with the j-th node within the k-th layer, $l_{ij}^{(k)} = -1$, otherwise $l_{ij}^{(k)} = 0$, and $l_{ii}^{(k)} = -\sum_{j=1}^{N} l_{ij}^{(k)}$, for $i, j = 1, 2, \cdots, N$ and $k = 1, 2, \cdots, M$. Similarly, if a node in the k-th layer is connected with its replica in the l-th layer, $d_{kl} = -1$, otherwise $d_{kl} = 0$, and $d_{kk} = -\sum_{l=1}^{M} d_{kl}$, for $k, l = 1, 2, \cdots, M$.

For simplicity, denote

$$\boldsymbol{x}^{(k)} = \begin{pmatrix} \boldsymbol{x}_1^{(k)} \\ \boldsymbol{x}_2^{(k)} \\ \vdots \\ \boldsymbol{x}_N^{(k)} \end{pmatrix}, \tilde{f}(\boldsymbol{x}^{(k)}) = \begin{pmatrix} f(\boldsymbol{x}_1^{(k)}) \\ f(\boldsymbol{x}_2^{(k)}) \\ \vdots \\ f(\boldsymbol{x}_N^{(k)}) \end{pmatrix}, \mathbf{x} = \begin{pmatrix} \boldsymbol{x}^{(1)} \\ \boldsymbol{x}^{(2)} \\ \vdots \\ \boldsymbol{x}^{(M)} \end{pmatrix}, F(\mathbf{x}) = \begin{pmatrix} \tilde{f}(\boldsymbol{x}^{(1)}) \\ \tilde{f}(\boldsymbol{x}^{(2)}) \\ \vdots \\ \tilde{f}(\boldsymbol{x}^{(M)}) \end{pmatrix},$$

then the evolution of the multiplex network (Eq. 1) can be rewritten as

$$\dot{\mathbf{x}} = F(\mathbf{x}) - c(\mathcal{L}^L \otimes H)\mathbf{x} - d(\mathcal{L}^I \otimes \Gamma)\mathbf{x}, \tag{2}$$

where $\mathcal{L}^L$ stands for the supra-Laplacian of intra-layer connections and $\mathcal{L}^I$ for the supra-Laplacian of inter-layer connections. In detail, $\mathcal{L}^L = \bigoplus_{l=1}^{M} L^{(k)} = \begin{pmatrix} L^{(1)} & & & \\ & L^{(2)} & & \\ & & \ddots & \\ & & & L^{(M)} \end{pmatrix}$ and $\mathcal{L}^I = L^I \otimes I_N$. Here $\bigoplus$ is the direct sum operation, I_N is the N-by-N identity matrix, $\otimes$ is the Kronecker product operation, $L^{(k)} = (l_{ij}^{(k)})_{N\times N}$ is the Laplacian matrix of nodes within the k-th layer, and $L^I = (d_{kl})_{M\times M}$ represents the inter-layer Laplacian matrix. More details about supra-Laplacians and multiplex network models can be found in Refs. [18, 23, 29, 31, 32] and references therein.

B. Three master stability equations

The master stability function method [25] is one of the most important methods to study stability of synchronized coupled identical systems. It simplifies a large-scale networked system to a node-size system via diagonalization and decoupling, as long as the inner coupling functions for all node pairs are identical. Thus, determining whether a network can reach synchronization can be turned into determining whether all the network characteristic modes fall into the corresponding synchronized regions. In the following, we will establish a master stability framework for multiplex networks with nonidentical inter-layer and intra-layer inner coupling functions.

According to the idea of the master stability framework [25], to investigate network synchronization, we can linearize the dynamical equation (2) at $\mathbf{1}_M \otimes \mathbf{1}_N \otimes \boldsymbol{s}$, where $\boldsymbol{s}$ is a synchronous state of the network satisfying $\dot{\boldsymbol{s}} = f(\boldsymbol{s})$ and $\mathbf{1}_M$ denotes an M-dimensional

vector with all entries being 1. We thus obtain the following variational equation:

$$\dot{\boldsymbol{\xi}} = [I_{M\times N} \otimes Df(\boldsymbol{s}) - c(\mathcal{L}^L \otimes H) - d(\mathcal{L}^I \otimes \Gamma)]\boldsymbol{\xi}, \tag{3}$$

where $\boldsymbol{\xi} = \mathbf{x} - \mathbf{1}_M \otimes \mathbf{1}_N \otimes \boldsymbol{s}$ and $I_{M\times N}$ is the identity matrix of order $M \times N$.

Suppose that $\mathcal{L}^L$ and $\mathcal{L}^I$ are symmetric matrices, and satisfy $\mathcal{L}^L\mathcal{L}^I = \mathcal{L}^I\mathcal{L}^L$. After diagonalization and decoupling (see Appendix B for details), we get the multiplex master stability equation for a system described by Eq. (1):

$$\dot{\boldsymbol{y}} = [Df(\boldsymbol{s}) - \alpha H - \beta\Gamma]\boldsymbol{y}, \tag{4}$$

where $\alpha = c\lambda$, $\beta = d\mu$, λ and μ are the eigenvalues of $\mathcal{L}^L$ and $\mathcal{L}^I$ respectively, and satisfy $\lambda^2 + \mu^2 \neq 0$.

Since this equation may be a time-varying system, particularly if $s(t)$ is a function of time, its eigenvalues may not be useful for determining the stability. Therefore, the largest Lyapunov exponent (LLE) of Eq. (4) is used instead, which is a function of α and β, denoted $\sigma(\alpha, \beta)$ and called the multiplex Master Stability Function for Eq. (1). Please see Appendix A for more information about Lyaponuv exponents.

When $\lambda \neq 0$ and $\mu = 0$, there is no inter-layer couplings regardless of d, for d arbitrarily chosen in $[0, +\infty)$, and Eq. (4) reduces to

$$\dot{\boldsymbol{y}} = [Df(\boldsymbol{s}) - \alpha H]\boldsymbol{y}, \tag{5}$$

It is clear that Eq. (5) becomes exactly the master stability equation of each independent intra-layer network (no inter-layer couplings).

Similarly, when $\lambda = 0$ and $\mu \neq 0$, we can obtain the following equation

$$\dot{\boldsymbol{y}} = [Df(\boldsymbol{s}) - \beta\Gamma]\boldsymbol{y}, \tag{6}$$

regardless of coupling strength c, for c arbitrarily chosen in $[0, +\infty)$. Eq. (6) becomes exactly the master stability equation for each independent inter-layer network (no intra-layer couplings).

For a single layer network, a necessary condition for the synchronization manifold to be stable is that the largest Lyapunov exponent $\sigma(\alpha)$ of Eq. (5) less than zero [38]. In analogy to a single layer, for the multiplex master stability equation (4), $\sigma(\alpha, \beta) < 0$ is a necessary condition for stability of the synchronization manifold in a multiplex network.

It is worth noting in particular the case when the intra- and inter-layer coupling functions are identical. Here $H = \Gamma$, and Eq. (4) turns into $\dot{\boldsymbol{y}} = [Df(\boldsymbol{s}) - \gamma H]\boldsymbol{y}$, (with $\gamma = \alpha + \beta$). This is the master stability equation for the corresponding single composite network where the inner coupling pattern (function) between any two nodes is identical, and a single supra-Laplacian can describe its topology. That is to say, the master stability equation of the single composite network is a special case of Eq. (4).

The assumption that $\mathcal{L}^L$ and $\mathcal{L}^I$ are symmetric and satisfy the commutativity condition is an important condition for decoupling the system and restricts our approach from applying to the full class of multiplex networks. But this assumption can be relaxed, as it is only a sufficient but not a necessary condition. First we consider the case when $\mathcal{L}^L$ and $\mathcal{L}^I$ are commutative but are nonsymmetric. As shown in AppendixE, the same master stability equations (4)-(6)(which correspond to Eqs. (E10), (E9) and (E6), respectively) can be derived provided that the multiplex network has intra-layer topology that is identical on each layer and that both the intra-layer Laplacian matrix L^L and the inter-layer Laplacian matrix L^I can be diagonalizable and have real eigenvalues. There are important classes of real-world networks that fit this paradigm, such as the Continuously Operating Reference Stations (CORS) geospatial information infrastructure [39–41] discussed in detail in Appendix F.

Next we consider the case when $\mathcal{L}^L$ and $\mathcal{L}^I$ do not commute. As shown in the simulation results with two-layer Rössler network with non-commutative supra-Laplacians, the three master stabilty equations (4)-(6) can be still used to predict network synchronization behaviors. In particular, for duplex networks, if the network topology is different on each layer, but there is one-to-one identical weighted coupling of nodes between layers, we can predict complete synchronization and intra-layer synchronization. If the topology on each layer is identical, but the one-to-one weighted coupling is not identical, we can predict complete synchronization and inter-layer synchronization. (See the simulation part for full details.)

C. Synchronized regions

Using the multiplex master stability equations developed above, we can analyze three types of synchronization behaviors: complete synchronization, intra-layer synchronization and inter-layer synchronization. Here we define the regions that support each behavior and

in the subsequent sections and Supplemental Material we show that it is the overlap of these regions that determines the type of sychronization pattern displayed by a multiplex network.

For the full multiplex network, from the multiplex master stability equation (4) we can calculate the region

$$R_{\alpha,\beta} = \{(\alpha,\beta)|\sigma(\alpha,\beta) < 0\},$$

which is called the joint synchronized region (which supports complete synchronization of the network). Whenever $\sigma(\alpha,\beta) < 0$, perturbations transverse to the synchronization manifold die out, and the network is said to be synchronizable.

From Eq. (5), we can get the region for intra-layer synchronization. The region depends only on the value of the parameter α, but to later allow comparison across the full parameter space we explicitly include the parameter β in the definition of the region,

$$R_{\alpha,\beta}^{Intra} = \{(\alpha,\beta)|\,\sigma(\alpha) < 0\},$$

where $LLE(\alpha)$ is the largest Lyapunov exponent for master stability equation (5). Similarly, from Eq. (6), we obtain the region for inter-layer synchronization

$$R_{\alpha,\beta}^{Inter} = \{(\alpha,\beta)|\sigma(\beta) < 0\}.$$

We call these regions in the parameter space of $(\alpha \geq 0, \beta \geq 0)$ the corresponding synchronized regions with respect to α and β.

When the network topological structures are specified, we can determine λ and μ (the eigenvalues of $\mathcal{L}^L$ and $\mathcal{L}^I$) directly, and then the regions $R_{\alpha,\beta}$, $R_{\alpha,\beta}^{Intra}$ and $R_{\alpha,\beta}^{Inter}$ can be parameterized simply in terms of coupling strengths c and d, denoted by $R_{c,d}$, $R_{c,d}^{Intra}$ and $R_{c,d}^{Inter}$. We call these regions the corresponding synchronized regions with respect to couplings c and d.

III. TWO-LAYER NETWORK OF RÖSSLER OSCILLATORS

With the multiplex MSF framework developed, we now analyze in more depth a specific example of a two-layer network of Rössler oscillators and calculate the different types of synchronized regions.

The famous Rössler chaotic oscillator is described as

$$\begin{cases} \dot{x} = -y - z, \\ \dot{y} = x + ay, \\ \dot{z} = z(x - c) + b\,, \end{cases} \tag{7}$$

where $a = b = 0.2$ and $c = 9$. This is the function f in the multiplex network Eq. (1). That is, the state of each node in the network is a three-dimensional vector with each component evolving by Eq. (7). For inner coupling matrices H and Γ, we consider the family of choices that fit the simplest form $I_{ij} \in \mathbb{R}^{3\times3}$ (where $i, j = 1, 2, 3$), which represents a matrix whose (i, j)-element is one and other elements are zero. The inter-layer topology is set to be one-to-one connection, that is to say, each node in one layer is connected to a counterpart node in the other layer.

Next, we first give an outline of the intra-layer and inter-layer synchronization, and then calculate the parameterized regions of synchronization for the general (unknown) intra-layer topologies and demonstrate how to determine synchronized regions after specifying the intra-layer topologies in the final subsection.

A. Intra-layer and inter-layer synchronization

It is well known that complete synchronization means all the nodes in a network come to an identical state. But for multiplex networks, it is also very significant to study intra-layer synchronization and inter-layer synchronization. As shown in Fig. 1, intra-layer synchronization means all the nodes within each layer reach an identical state, while inter-layer synchronization means each node in a layer reaches the same state as its counterparts in other layers.

B. Synchronized regions for unknown intra-layer topologies

The regions of synchronization calculated from the multiplex MSF are parameterized by α and β, and thus do not require that the inter- and intra-layer topology are specified. Figure 2 shows the synchronized regions as parameterized by (α, β) for a two-layer multiplex network of Rössler oscillators with arbitrary topology for different combinations of inter-layer and intra-layer coupling matrices H and Γ. Here, the green (grey) shading represents the regions

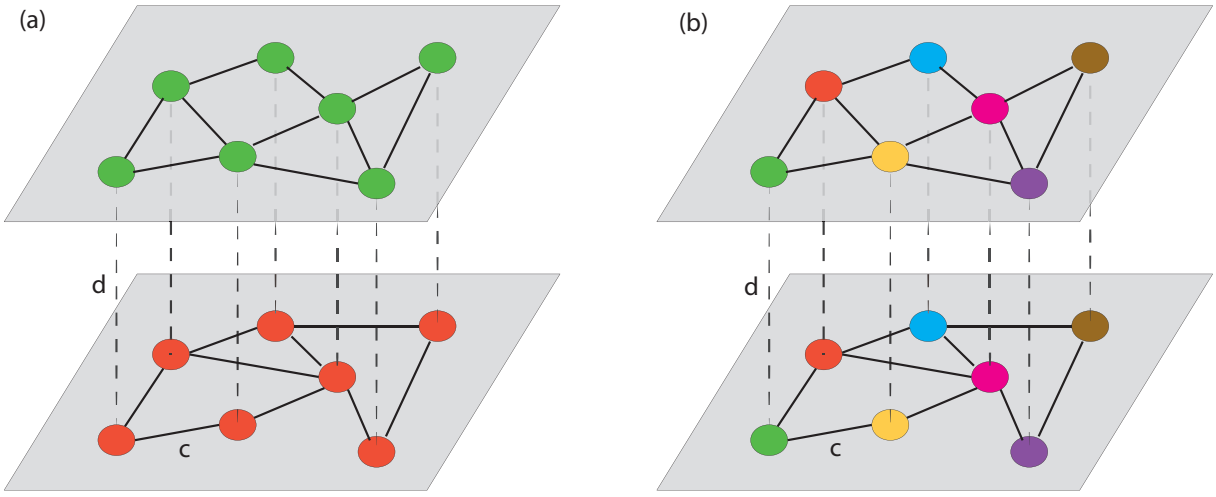

FIG. 1. Schematic representation of (a) intra-layer synchronization and (b) inter-layer synchronization, in a multiplex network of two layers.

$R_{\alpha,\beta}$ as obtained from the master stability equation (4). The regions $R^{Intra}_{\alpha,\beta}$ as obtained from Eq. (5) are enclosed by the dash-dotted blue lines, and the regions $R^{Inter}_{\alpha,\beta}$ as obtained from Eq. (6) enclosed by the dashed red lines.

Synchronization occurs in the region when the MSF criterion is negative, in other words when $\sigma(\alpha,\beta) < 0$. Thus from Fig. 2, we can easily obtain the joint synchronized region:

$$R_{\alpha,\beta} \approx \{(\alpha,\beta)|\, 0.2 < \alpha+\beta < 4.6\} \quad \text{for } H = I_{11} \text{ and } \Gamma = I_{11},$$

$$R_{\alpha,\beta} \approx \{(\alpha,\beta)|\, 0.23 < \alpha < 4.3, \beta \geq 0\} \quad \text{for } H = I_{11} \text{ and } \Gamma = I_{13},$$

$$R_{\alpha,\beta} \approx \{(\alpha,\beta)|\, \frac{\alpha}{0.2} + \frac{\beta}{0.18} > 1, \beta > h(\alpha)\} \quad \text{for } H = I_{11} \text{ and } \Gamma = I_{22}$$

$$R_{\alpha,\beta} \approx \{(\alpha,\beta)|\, \beta > 0.2, \alpha \geq 0\} \quad \text{for } H = I_{13} \text{ and } \Gamma = I_{22},$$

where $h(\alpha) = -10^{-5}\alpha^4 + 0.00057\alpha^3 - 0.012\alpha^2 + 0.12\alpha - 0.35$.

In particular, letting $\beta = 0$ in $R_{\alpha,\beta}$, we have the interval $R_\alpha = (0.2,\, 4.6)$ for $H = I_{11}$, $R_\alpha = \emptyset$ for $H = I_{13}$, and $R_\alpha = (0.18,\, \infty)$ for $H = I_{22}$. Similarly, letting $\alpha = 0$ in $R_{\alpha,\beta}$, we have $R_\beta = (0.2,\, 4.6)$ for $\Gamma = I_{11}$, $R_\beta = \emptyset$ for $\Gamma = I_{13}$, and $R_\beta = (0.18,\, \infty)$ for $\Gamma = I_{22}$. Here, the intervals $R_\alpha \triangleq \{\alpha|\, \sigma(\alpha) < 0\}$ and $R_\beta \triangleq \{\beta|\, \sigma(\beta) < 0\}$ can also be obtained from Eqs. (5) and (6), respectively.

Consequently, for three types of coupling patterns, i.e., $H = I_{11}$ and any Γ, $H = I_{13}$ and any Γ, and $H = I_{22}$ and any Γ, we get the following region for intra-layer synchronization,

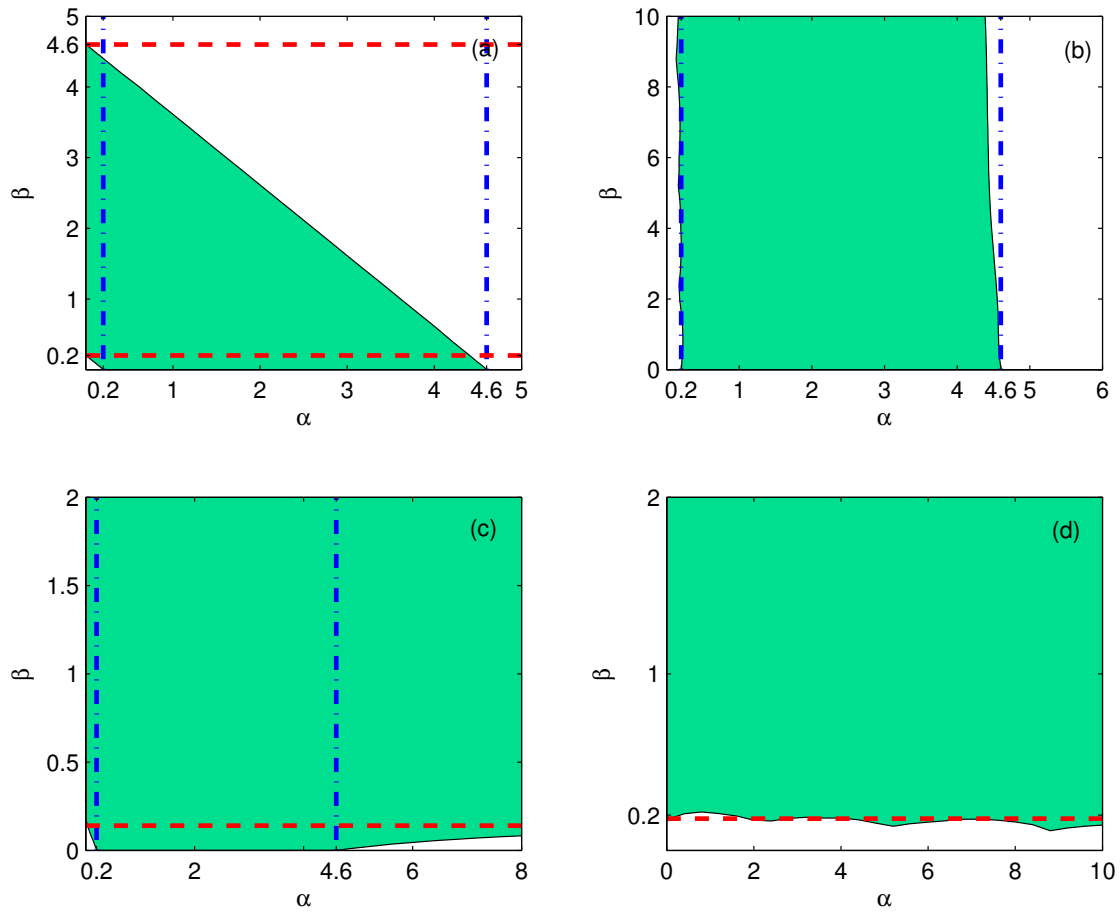

FIG. 2. The synchronized regions with respect to α and β, $R_{\alpha,\beta}$ painted with green (grey) color, $R^{Intra}_{\alpha,\beta}$ enclosed by the dash-dotted blue lines, and $R^{Inter}_{\alpha,\beta}$ enclosed by the dashed red lines. Here the Rössler oscillator is taken as nodal dynamics, and the intra-layer coupling matrix H and the inter-layer coupling matrix Γ are chosen as follows: (a) $H = I_{11}$, $\Gamma = I_{11}$, (b) $H = I_{11}$, $\Gamma = I_{13}$, (c) $H = I_{11}$, $\Gamma = I_{22}$, (d) $H = I_{13}$, $\Gamma = I_{22}$.

respectively.

$$R^{Intra}_{\alpha,\beta} = \{(\alpha,\beta)|\, 0.2 < \alpha < 4.6,\ \beta \geq 0\},\ R^{Intra}_{\alpha,\beta} = \emptyset,$$

and

$$R^{Intra}_{\alpha,\beta} = \{(\alpha,\beta)|\, 0.18 < \alpha < +\infty,\ \beta \geq 0\}.$$

Analogously, we can obtain $R^{Inter}_{\alpha,\beta}$ by replacing α with β, and H with Γ in the above $R^{Intra}_{\alpha,\beta}$.

As shown in Fig. 2, for $H = I_{11}$ and $\Gamma = I_{11}$, the regions

$$R^{Intra}_{\alpha,\beta} = \{(\alpha,\beta)|\, 0.2 < \alpha < 4.6,\ \beta \geq 0\} \text{ and } R^{Inter}_{\alpha,\beta} = \{(\alpha,\beta)|\, 0.2 < \beta < 4.6,\ \alpha \geq 0\},$$

which are enclosed by the dash-dotted blue and dashed red lines, respectively.

For $H = I_{11}$ and $\Gamma = I_{13}$,

$$R_{\alpha,\beta}^{Intra} = \{(\alpha,\beta)|\, 0.2 < \alpha < 4.6,\, \beta \geq 0\}, \text{ and } R_{\alpha,\beta}^{Inter} = \emptyset,$$

where $R_{\alpha,\beta}^{Intra}$ is enclosed by the dash-dotted blue lines.

For $H = I_{11}$ and $\Gamma = I_{22}$, $R_{\alpha,\beta}^{Intra}$ is the part enclosed by the dash-dotted blue lines, and $R_{\alpha,\beta}^{Inter}$ is the one above the dashed red line. To be exact,

$$R_{\alpha,\beta}^{Intra} = \{(\alpha,\beta)|\, 0.2 < \alpha < 4.6,\, \beta \geq 0\} \text{ and } R_{\alpha,\beta}^{Inter} = \{(\alpha,\beta)|\, 0.18 < \beta < +\infty,\, \alpha \geq 0\}.$$

For $H = I_{13}$ and $\Gamma = I_{22}$, $R_{\alpha,\beta}^{Intra} = \emptyset$, and $R_{\alpha,\beta}^{Inter} = \{(\alpha,\beta)|\, 0.18 < \beta < +\infty,\, \alpha \geq 0\}$, which is above the dashed red line.

Generally speaking, a multiplex network with a specified topology can achieve complete synchronization when all the nonzero network characteristic modes, including those of the intra-layer and inter-layer Laplacians, fall into the synchronized region. For a two-layer network with identical intra-layer topologies, our theoretical analysis (see Appendix E) further shows that a duplex network can achieve complete synchronization when all the nonzero characteristic modes fall into the intersection of $R_{\alpha,\beta}$, $R_{\alpha,\beta}^{Intra}$ and $R_{\alpha,\beta}^{Inter}$. Therefore, according to the overlapping region, one can determine whether the network achieves complete synchronization or not after specifying the topology. However, what happens when all the nonzero characteristic modes do not fall into the intersection? Further simulations shows that in this case the network could support other coherent dynamical behaviors, such as intra-layer or inter-layer synchronization.

C. Synchronized regions with given intra-layer topologies

To push the analysis further, we must specify the topology of the two-layer Rössler oscillator network. For simplicity, assume that the two layers have the same intra-layer topology, and each node in one layer is connected with its replica in the other layer. Consider that each layer is a star network consisting of 5 nodes. Then, the intra-layer Laplacian matrix

is

$$L = \begin{pmatrix} 4 & -1 & -1 & -1 & -1 \\ -1 & 1 & 0 & 0 & 0 \\ -1 & 0 & 1 & 0 & 0 \\ -1 & 0 & 0 & 1 & 0 \\ -1 & 0 & 0 & 0 & 1 \end{pmatrix},$$

and the intra-layer supra-Laplacian matrix is $\mathcal{L}^L = \begin{pmatrix} L & 0 \\ 0 & L \end{pmatrix}$. The inter-layer Laplacian matrix $L^I = \begin{pmatrix} 1 & -1 \\ -1 & 1 \end{pmatrix}$, and the inter-layer supra-Laplacian matrix $\mathcal{L}^I = L^I \otimes I_5$. It is easy to verify that $\mathcal{L}^L\mathcal{L}^I = \mathcal{L}^I\mathcal{L}^L$, and the characteristic values of $\mathcal{L}^L$ and $\mathcal{L}^I$ are $\lambda =$ 0, 0, 1, 1, 1, 1, 1, 1, 5, 5 and $\mu = 0$, 0, 0, 0, 0, 2, 2, 2, 2, 2, respectively.

We can calculate the eigenvalues λ and μ directly and parameterize the synchronized regimes by the coupling strengths c and d (rather than the more general α and β) for all the different combinations of the inner coupling matrices H and Γ. (See Appendix B for more details on transforming $R_{\alpha,\beta}$ to $R_{c.d}$.) Consequently, for $H = I_{11}$ and $\Gamma = I_{11}$, the region with respect to parameters c and d is

$$R_{c,d} \approx \{(c,d)|\, 0.2 < c + 2d, c + 0.4d < 0.92\}.$$

Similarly, for $H = I_{11}$ and $\Gamma = I_{13}$, then

$$R_{c,d} \approx \{(c,d)|\, 0.23 < c < 0.86, d \geq 0\};$$

for $H = I_{11}$ and $\Gamma = I_{22}$, then

$$R_{c,d} \approx \{(c,d)|\, \frac{c}{0.2} + \frac{d}{0.09} > 1, d > h(c)\}$$

where $\frac{1}{2}(-625 \cdot 10^{-5}c^4 + 0.07125c^3 - 0.2c^2 + 0.6c - 0.35)$; and for $H = I_{13}$ and $\Gamma = I_{22}$, then $R_{c,d} \approx \{(c,d)|\, d > 0.1, c \geq 0\}$. These regions, $R_{c,d}$, are shown in Figs. 3-6 by the solid lines in panels (c) for the different choices of H and Γ considered.

To test our theoretical predictions we next numerically solve the duplex Rössler networked system, and identify the parameter regions that support the three different coherent behaviors: complete synchronization, intra-layer synchronization and inter-layer synchronization.

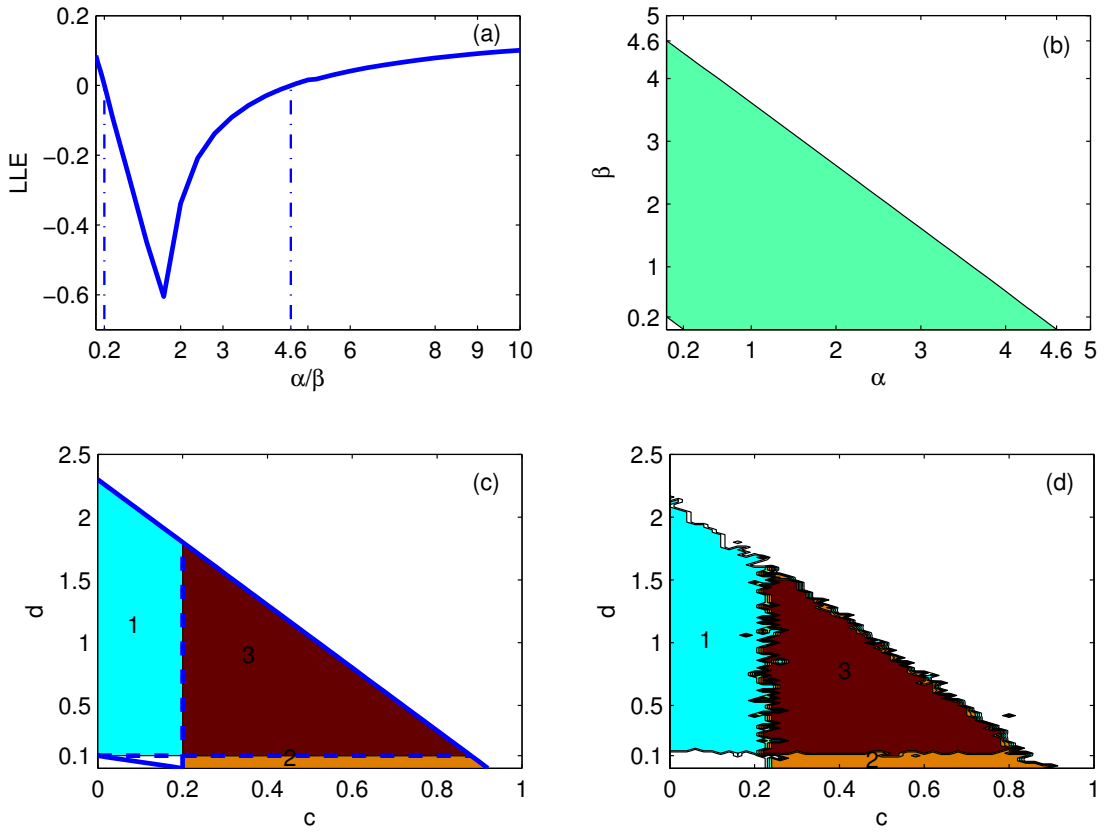

FIG. 3. Network synchronized regions for $H = I_{11}$ and $\Gamma = I_{11}$. (a) the synchronized interval of the independent intra-layer/inter-layer Rössler network with respect to α/β; (b) the synchronized region with respect to α and β for Rössler networks; (c) the synchronized region with respect to couplings c and d for a Rössler duplex consisting of two star layers with one-to-one inter-layer connections; (d) numerical synchronization areas with respect to couplings c and d, in which the maroon (deep grey) region represents complete synchronization area, the yellow (medium grey) is for intra-layer synchronization, and the cyan (light grey) is inter-layer synchronization and the white region represents non-synchronization.

We quantify that the system has reached the specific type of behavior via the synchronization errors as defined in Appendix D. By bounding the values of these errors we develop three different indicator functions, which identify that the system has achieved macroscopic order of the form: $I_d = 3$ when the network reaches complete synchronization, $I_d = 2$ for intra-layer synchronization, $I_d = 1$ for inter-layer synchronization and $I_d = 0$ for none of the above cases. See Appendix D for full details.

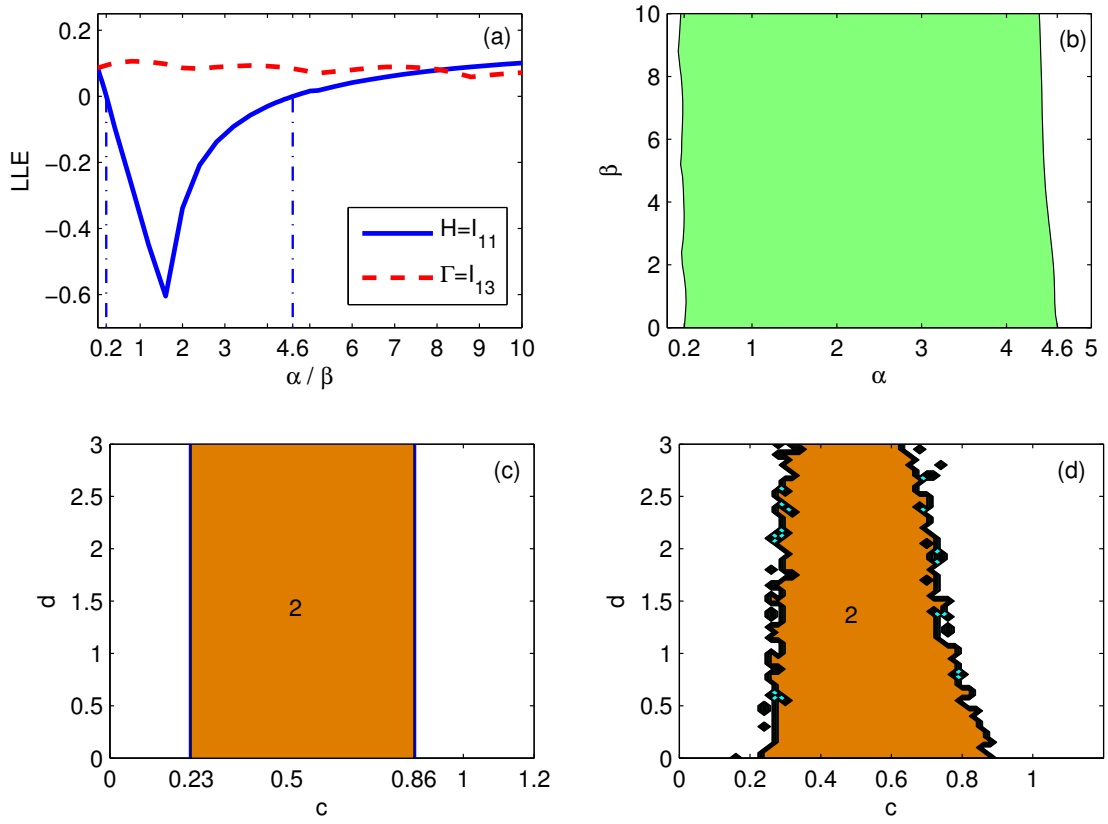

FIG. 4. Network synchronized regions for $H = I_{11}$ and $\Gamma = I_{13}$. (a) the synchronized interval of the independent intra-layer/inter-layer Rössler network with respect to α/β; (b) the synchronized region with respect to α and β for Rössler networks; (c) the synchronized region with respect to couplings c and d for a Rössler duplex consisting of two star layers with one-to-one inter-layer connections; (d) numerical synchronization areas with respect to couplings c and d, in which the maroon (deep grey) region represents complete synchronization area, the yellow (medium grey) is for intra-layer synchronization, and the cyan (light grey) is inter-layer synchronization and the white region represents non-synchronization.

Figure 3 shows network synchronized regions for the two-layer star network of Rössler oscillators for the scenario $H = I_{11}$ and $\Gamma = I_{11}$. In detail, panel (a) displays the synchronized intervals of the independent intra-layer and inter-layer Rössler networks with respect to α or β, which can be calculated from the master stability equations (5) and (6) (without consideration of d or c), respectively. Since $H = \Gamma$, the two intervals overlap. Panel (b) gives the synchronized region with respect to α and β for this Rössler network calculated

from the master stability equation (4). Panel (c) shows the synchronized region as a function of intra- and inter-layer coupling strength c and d. Panel (d) shows the numerically calculated indicator function (i.e., the numerically calculated values of synchronization error as classified in Eq. (D4) given in Appendix D) with respect to couplings c and d for this duplex Rössler network. Here the maroon (deep grey) area labeled with '3' represents complete synchronization, the yellow (medium grey) area labeled with '2' is for intra-layer synchronization, the cyan (light grey) label with '1' is for inter-layer synchronization, and the white region represents cases otherwise.

Other choices for the coupling functions H and Γ are shown in Figures 4-6 for this same two-layer star network of Rössler oscillators. The results are analogous to those in Fig. 3. It is worth noting that in panels (c) of all of these figures the regions of complete, intra-layer and inter-layer synchronization predicted by the multiplex MSF Eqs. (4) to (6), shown as the maroon (deep grey), yellow (medium grey) and cyan (light grey) regions respectively, can capture all of the behaviors exhibited by direct numerical simulations shown in panels (d).

Next we show how these distinct areas can be determined from the three regions: $R_{c,d}$, $R_{c,d}^{Intra}$, and $R_{c,d}^{Inter}$ derived from Eqs. (4), (5), and (6). As a matter of fact, the intersections of the regions determine the type of coherent behavior that is stable. Specifically, the intersection of all the three regions determines complete synchronization, the intersection of $R_{c,d}$ and $R_{c,d}^{Intra}$ determines intra-layer synchronization, and the intersection of $R_{c,d}$ and $R_{c,d}^{Inter}$ determines inter-layer synchronization.

For example, for the case with $H = I_{11}$ and $\Gamma = I_{11}$, the synchronized region $R_{c,d} = \{(c,d)|\, c + 2d > 0.2, c + 0.4d < 0.92\}$, the intra-layer synchronized region $R_{c,d}^{Intra} = \{(c,d)|\, 0.2 < c < 0.92,\, d \geq 0\}$ and the inter-layer synchronized region $R_{c,d}^{Inter} = \{(c,d)|c \geq 0,\, 0.1 < d < 2.3\,\}$. The intersection of these three parts is $\{(c,d)|\, c > 0.2,\ d > 0.1,\ c+0.4d < 0.92\}$, as labeled by number '3' in panel (c) of Fig. 3, which essentially coincides with the numerically calculated complete synchronization area in maroon (deep grey) color in panel (d). Furthermore, the mere intra-layer synchronization (without inter-layer synchronization) area in yellow (medium grey) in panel (d) coincides with the region labeled as '2' in panel (c): $R_{c,d} \cap R_{c,d}^{Intra} - R_{c,d}^{Inter} = \{(c,d)|\, c > 0.2, 0 \leq d < 0.1,\, c + 0.4d < 0.92\}$, and the mere inter-layer synchronization (without intra-layer synchronization) area in cyan (light grey) agrees well with the region labeled as '1' in panel (c): $R_{c,d} \cap R_{c,d}^{Inter} - R_{c,d}^{Intra} = \{(c,d)|\, 0 \leq$

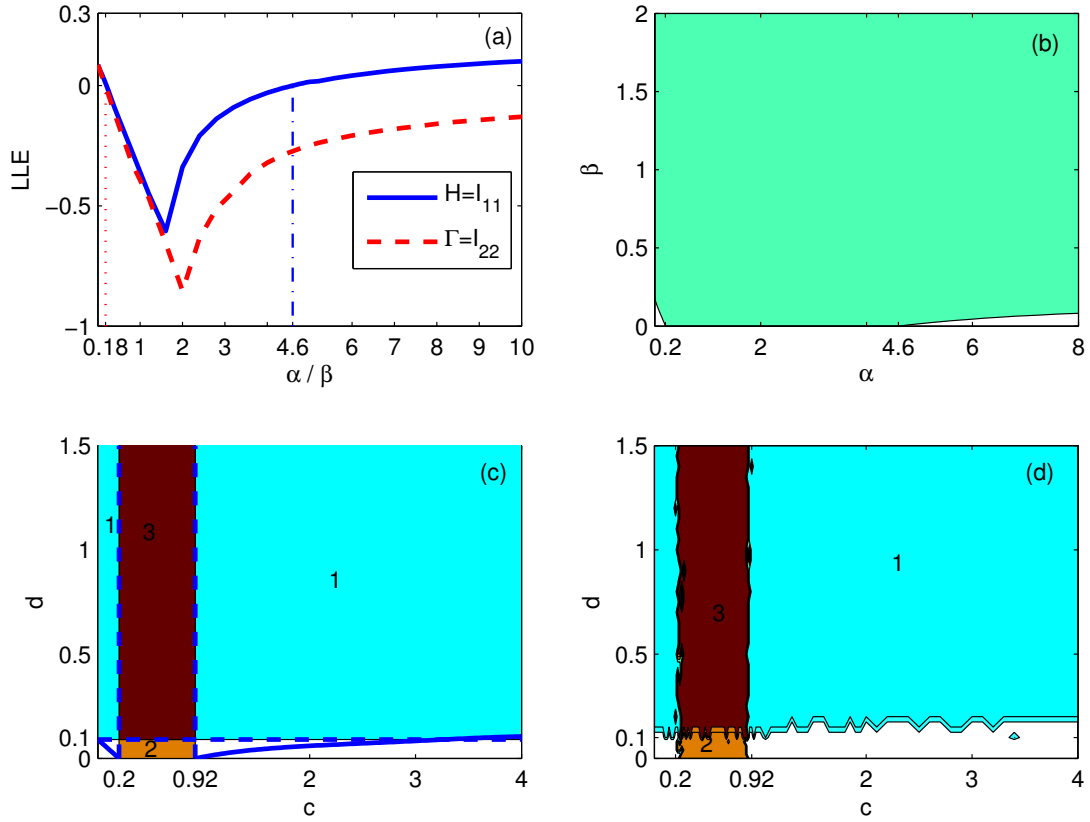

FIG. 5. Network synchronized regions for $H = I_{11}$ and $\Gamma = I_{22}$. (a) the synchronized interval of the independent intra-layer/inter-layer Rössler network with respect to α/β; (b) the synchronized region with respect to α and β for Rössler networks; (c) the synchronized region with respect to couplings c and d for a Rössler duplex consisting of two star layers with one-to-one inter-layer connections; (d) numerical synchronization areas with respect to couplings c and d, in which the maroon (deep grey) region represents complete synchronization area, the yellow (medium grey) is for intra-layer synchronization, and the cyan (light grey) is inter-layer synchronization and the white region represents non-synchronization.

$c < 0.2$, $d > 0.1$, $c + 0.4d < 0.92\}$. Similar observations can be obtained in panels (c) and (d) of Figs. 4-6.

In other words, the actual area for complete synchronization is determined by the intersection of $R_{c,d}$, $R_{c,d}^{Intra}$ and $R_{c,d}^{Inter}$, that is, $R_{c,d} \cap R_{c,d}^{Intra} \cap R_{c,d}^{Inter}$. Moreover, the mere intra-layer synchronization area is determined by the intersection of synchronized region and intra-layer snchronized region subtracting the inter-layer synchronized part, that is, $R_{c,d} \cap R_{c,d}^{Intra} - R_{c,d}^{Inter}$.

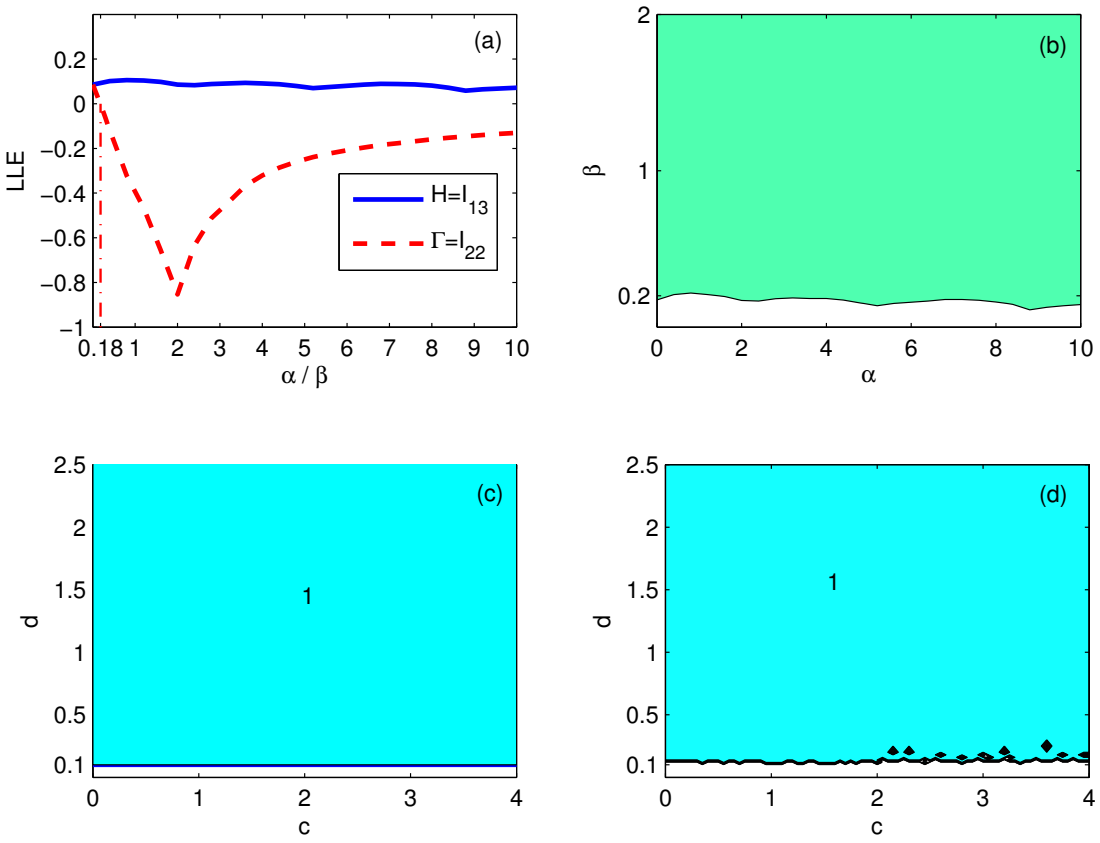

FIG. 6. Network synchronized regions for $H = I_{13}$ and $\Gamma = I_{22}$. (a) the synchronized interval of the independent intra-layer/inter-layer Rössler network with respect to α/β; (b) the synchronized region with respect to α and β for Rössler networks; (c) the synchronized region with respect to couplings c and d for a Rössler duplex consisting of two star layers with one-to-one inter-layer connections; (d) numerical synchronization areas with respect to couplings c and d, in which the maroon (deep grey) region represents complete synchronization area, the yellow (medium grey) is for intra-layer synchronization, and the cyan (light grey) is inter-layer synchronization and the white region represents non-synchronization.

The mere inter-layer synchronization area is determined by $R_{c,d} \cap R_{c,d}^{Inter} - R_{c,d}^{Intra}$.

Furthermore, when nodal dynamics and network structures are given, $R_{c,d}^{Intra}$ and $R_{c,d}^{Inter}$ are mainly determined by the inner coupling matrices of the intra-layer nodes (H) and the inter-layer nodes (Γ) respectively, and $R_{c,d}$ is determined by both. Particularly, if the inter-layer coupling matrix Γ makes the inter-layer synchronized region $R_{c,d}^{Inter}$ empty, then the multiplex network cannot achieve inter-layer synchronization, resulting in the failure of

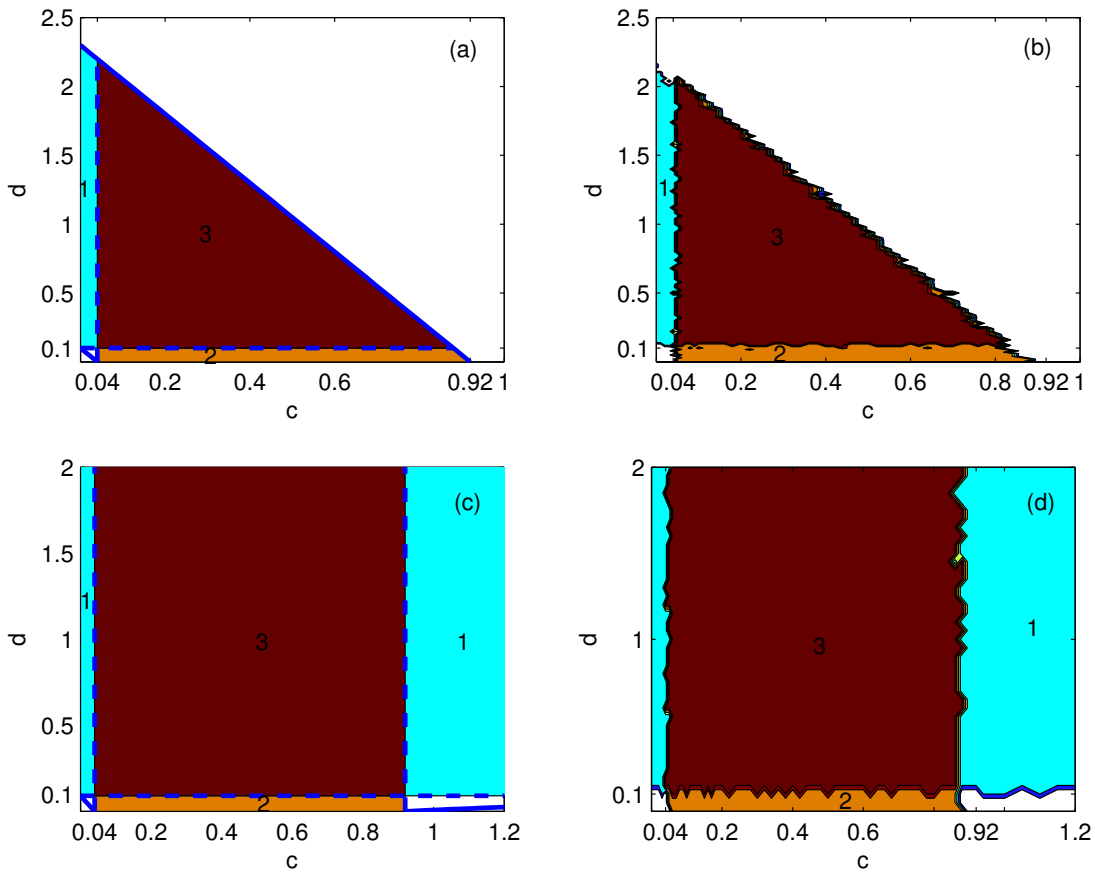

FIG. 7. Network synchronized regions for Rössler networks composed of two single-layer fully connected networks with different H and Γ, $H = I_{11}, \Gamma = I_{11}$ for (a) and (b), and $H = I_{11}, \Gamma = I_{22}$ (c) and (d). (a) and (c) are the synchronized regions about c and d; (b) and (d) are respectively corresponding numerical synchronization areas, in which the maroon (deep grey) region represents complete synchronization area, the yellow (medium grey) is for intra-layer synchronization, and the cyan (light grey) is inter-layer synchronization and the white region represents non-synchronization.

complete synchronization, as shown in Fig. 4. If the intra-layer coupling matrix H makes the intra-layer synchronized region $R_{c,d}^{Intra}$ empty, then the multiplex network cannot achieve intra-layer synchronization, which also leads to failure of complete synchronization, as shown in Fig. 6.

In order to verify the previous results on a different multiplex topology, we consider a duplex network composed of two fully connected network layers with one-to-one inter-layer connections. The results shown in Figs. 7 and 8 again illustrate the above observations.

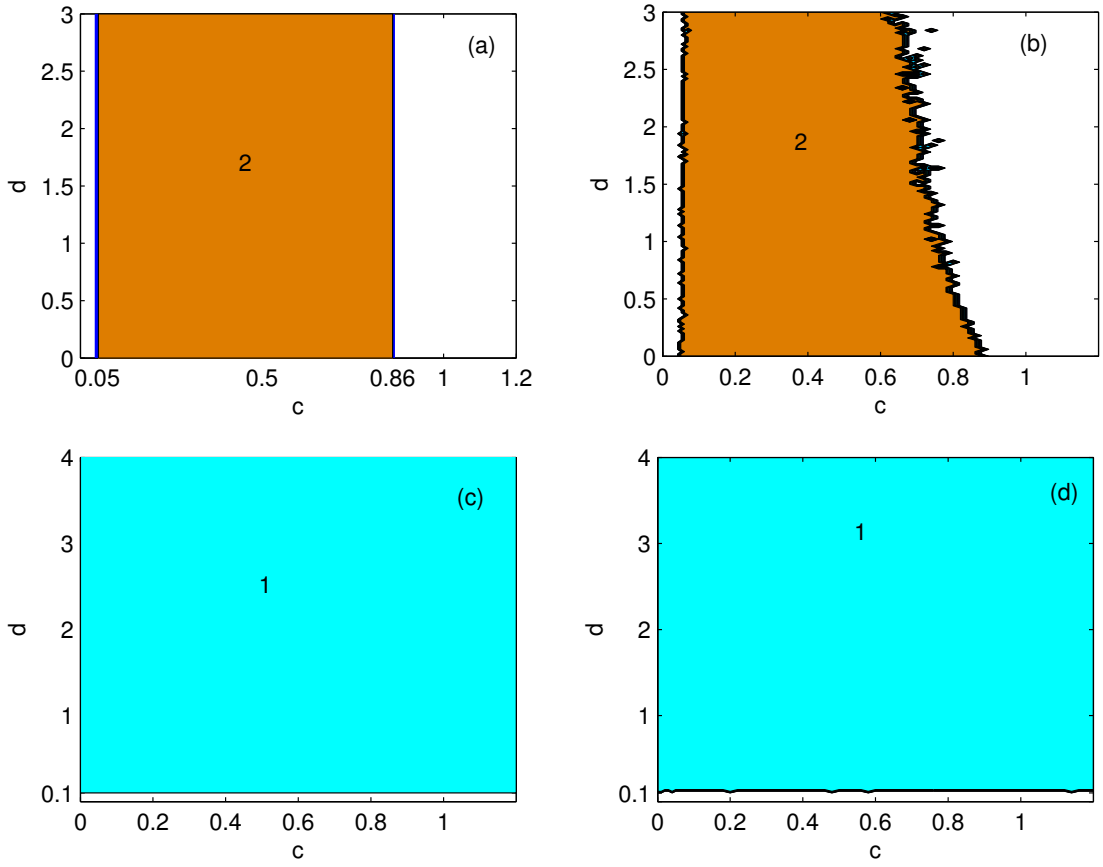

FIG. 8. Network synchronized regions for Rössler networks composed of two single-layer fully connected networks with different H and Γ, $H = I_{11}, \Gamma = I_{13}$ for (a) and (b), and $H = I_{13}, \Gamma = I_{22}$ (c) and (d). (a) and (c) are the synchronized regions about c and d; (b) and (d) are respectively corresponding numerical synchronization areas, in which the maroon (deep grey) region means mere complete synchronization, the yellow (medium grey) region means mere intra-layer synchronization, the cyan (light grey) region means inter-layer synchronization and the blue region means non-synchronization.

IV. TWO-LAYER RÖSSLER NETWORK WITH NON-COMMUTATIVE SUPRA-LAPLACIANS

So far we have analyzed the case of commutative supra-Laplacians with which we derive the three master stability equations (4)-(6). However, the commutativity condition restricts our approach from applying to the full class of multiplex networks, it is only a sufficient but not a necessary condition, and can be relaxed.

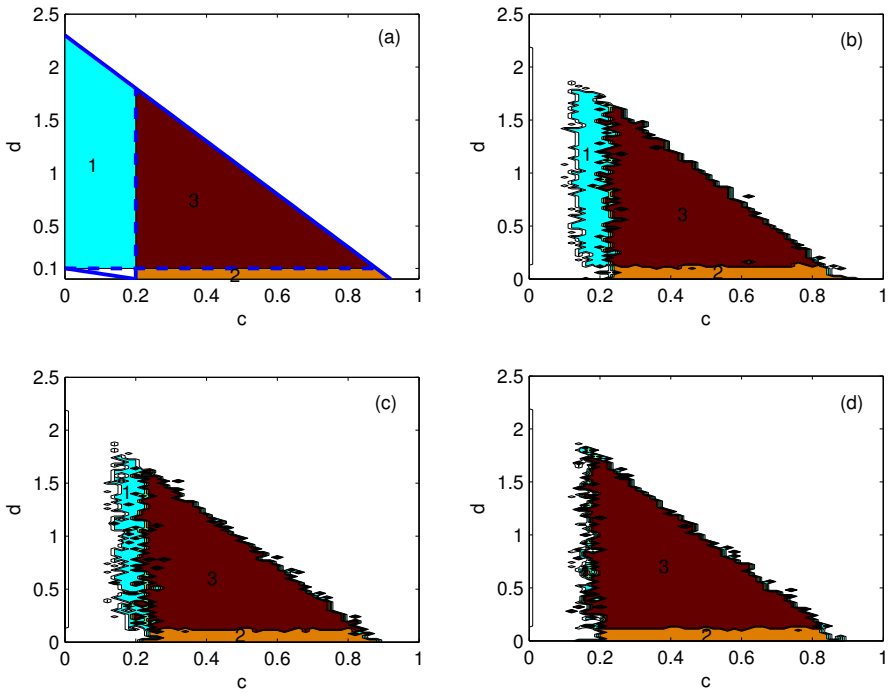

FIG. 9. The case of non-commutative supra-Laplacian matrices with different intra-layer topologies and identical inter-layer coupling weights. Network synchronized regions calculated from master stability equations (a) and the numerical synchronization areas (b)(c)(d) for $H = I_{11}$ and $\Gamma = I_{11}$. The first layer of the duplex network is the star-type, the second layer is the one generated from the star-type with 1 (b), 2 (c) and 3 (d) additional edges , respectively. The one-to-one coupling between layers is identical.

Here we consider two cases of non-commutative supra-Laplacians for showing that the three master stability equations can be still used to predict network synchronization behaviors. one is a duplex network that has different topology on each layer and one-to-one identical weighted coupling of nodes between layers. The other is a duplex network that has identical topology on each layer and one-to-one nonidentical weighted coupling of nodes between layers.

For the first case, consider specific duplex networks with 5 nodes on each layer and one-to-one coupling of nodes between layers, where one layer is the star-type, and the other is the star-type with 1, 2 or 3 additional edges. In this case, it is easy to verify that the intra- and inter-layer supra-Laplacian matrices $\mathcal{L}^L = \begin{pmatrix} L_1 & 0 \\ 0 & L_2 \end{pmatrix}$ and $\mathcal{L}^I = L^I \otimes I_N$ do not

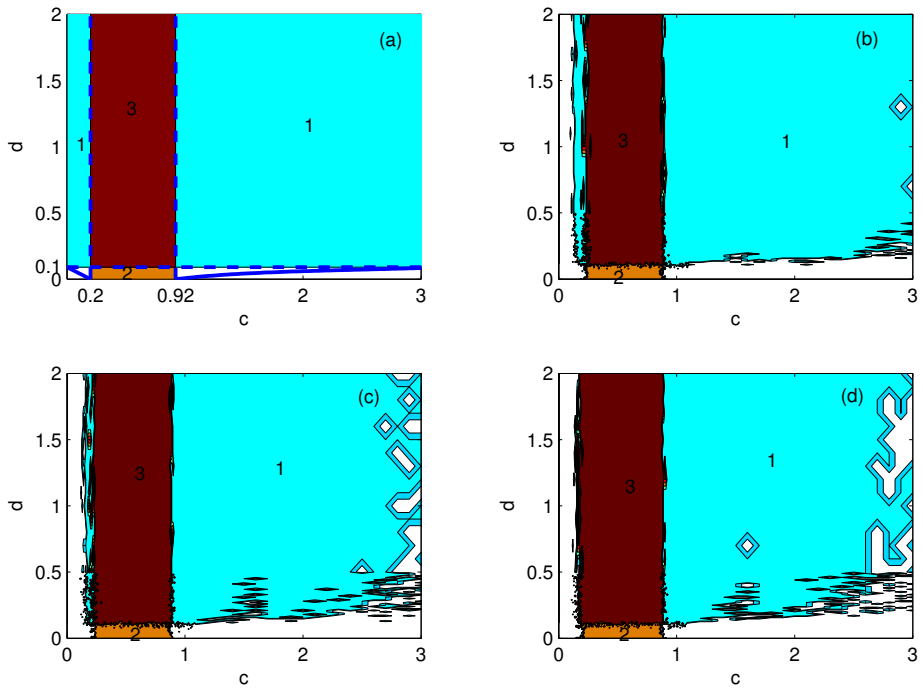

FIG. 10. The case of non-commutative supra-Laplacian matrices with different intra-layer topologies and identical inter-layer coupling weights. Network synchronized regions calculated from master stability equations (a) and the numerical synchronization areas (b)(c)(d) for $H = I_{11}$ and $\Gamma = I_{22}$. The first layer of the duplex network is the star-type, the second layer is the one generated from the star-type with 1 (b), 2 (c) and 3 (d) additional edges , respectively. The one-to-one coupling between layers is identical.

commute. Here $L^I = \begin{pmatrix} 1 & -1 \\ -1 & 1 \end{pmatrix}$, and the smallest nonzero eigenvalues of the two intra-layer Lapacian matrices L_1 and L_2 are equal and their largest eigenvalues are also equal, i.e. $\lambda_2 = 1$ and $\lambda_N = 5$.

For the second case, consider specific duplex networks that have identical star-type or fully-connected topology on each layer, and nonidentical weighted one-to-one coupling between layers, with the inter-layer supra-Lapalacian matrix being $\mathcal{L}^I = L^I \otimes \mathrm{diag}\{2, 1, 1, 1, 1\}$, where here $L^I = \begin{pmatrix} 1 & -1 \\ -1 & 1 \end{pmatrix}$. In this case, $\mathcal{L}^I$'s smallest nonzero eigenvalue $\mu_2 = 2$ and its largest eigenvalue $\mu_N = 4$. It is easy to verify that $\mathcal{L}^L$ and $\mathcal{L}^I$ do not commute.

Figures 9–12 show results for the above two different classes of duplex networks with different combinations of H and Γ. We still find that the overlapping regions obtained from

the three master stability equations closely coincide with the numerically calculated areas for the three different types of synchronous behaviors. Specifically, the actual area for complete synchronization is determined by $R_{c,d} \cap R_{c,d}^{Intra} \cap R_{c,d}^{Inter}$ for both classes of non-commutative supra-Laplacians. For duplex networks with different intra-layer topologies (the first class), the intra-layer synchronization area is determined by $R_{c,d} \cap R_{c,d}^{Intra}$. For duplex networks with nonidentical weighted one-to-one coupling (the second class), the inter-layer synchronization area is determined by $R_{c,d} \cap R_{c,d}^{Inter}$. These findings shed light on the significant facts that the difference of the intra-layer topologies can lead to the change of the actual inter-layer synchronized regions, and nonidentical inter-layer one-to-one coupling weights can lead to the change of the actual intra-layer synchronized regions.

In other words, even though here the inter- and intra-layer supra-Laplacian matrices do not commute, the three synchronized regions still predict the actual areas for complete synchronization and intra-layer synchronization, or for complete synchronization and inter-layer synchronization. Therefore, the commutation condition is not necessary for our findings, it is only sufficient for our theoretical analysis. Particularly for the case of different intra-layer topologies, one can apply these three synchronized regions to predict the actual areas for complete synchronization and intra-layer synchronization. How generally the observation applies remains an open question.

V. A THREE-LAYER NETWORK OF RÖSSLER OSCILLATORS

Here, consider a three-layer network of Rössler oscillators with identical internal topology (such as the fully-connected structure) and chain-type coupling between layers. That is, the intra-layer supra-Laplacian matrix $\mathcal{L}^L = I_3 \otimes L$, and the inter-layer supra-Laplacian matrix $\mathcal{L}^L = L^I \otimes I_N$, where $L^I = \begin{pmatrix} 1 & -1 & 0 \\ -1 & 2 & -1 \\ 0 & -1 & 1 \end{pmatrix}$.

As shown in Figs. 13 and 14, the three synchronized regions calculated from the three master stability equations can also predict the actual areas for the three synchronous behaviors, further verifying that our findings can apply beyond duplex networks.

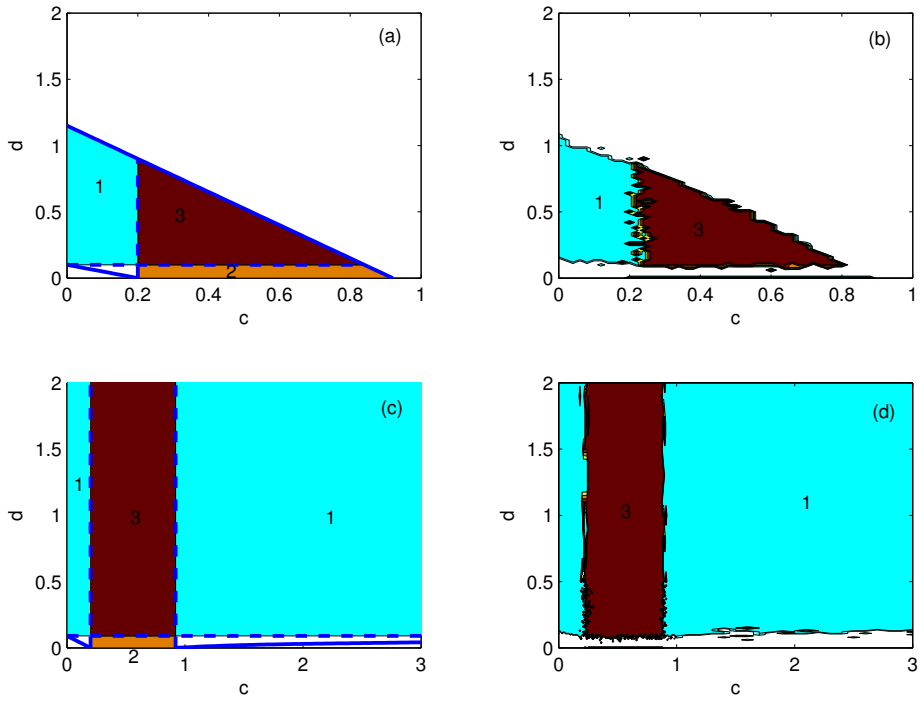

FIG. 11. The case of non-commutative supra-Laplacian matrices. Network synchronized regions from master stability equations (left) and numerical synchronization areas (right) for Rössler networks with identical star-type intra-layer topologies and nonidentical one-to-one coupling weights between layers. Here the inter-layer supra-Laplacian matrix $\mathcal{L}^I = [1 \ \ -1; -1 \ \ 1] \otimes \mathrm{diag}\{2,1,1,1,1\}$, $H = I_{11}$ and $\Gamma = I_{11}$ for (a)(b), and $H = I_{11}$ and $\Gamma = I_{22}$ for (c)(d).

VI. DISCUSSION

In summary, we develop a master stability function framework which captures an essential feature of multiplex networks, that the intra-layer and inter-layer coupling functions can be distinct. Here we define a distinct supra-Laplacian matrix for intra-layer connections, denoted $\mathcal{L}^L$, and one for inter-layer connections, denoted $\mathcal{L}^I$. If $\mathcal{L}^L$ and $\mathcal{L}^I$ commute, the multiplex network can be easily decoupled and thus the characteristic modes of the intra-layer Laplacian are separated from those of the inter-layer one. (Note this commutation condition is a sufficient but not a necessary condition for our theoretical analysis. See Sec. IV for details.) We can then develop a multiplex master stability equation, Eq. (4), to establish the necessary region for complete synchronization. In the limit of no inter-layer coupling the multiplex MSF reduces to a master stability equation for each independent

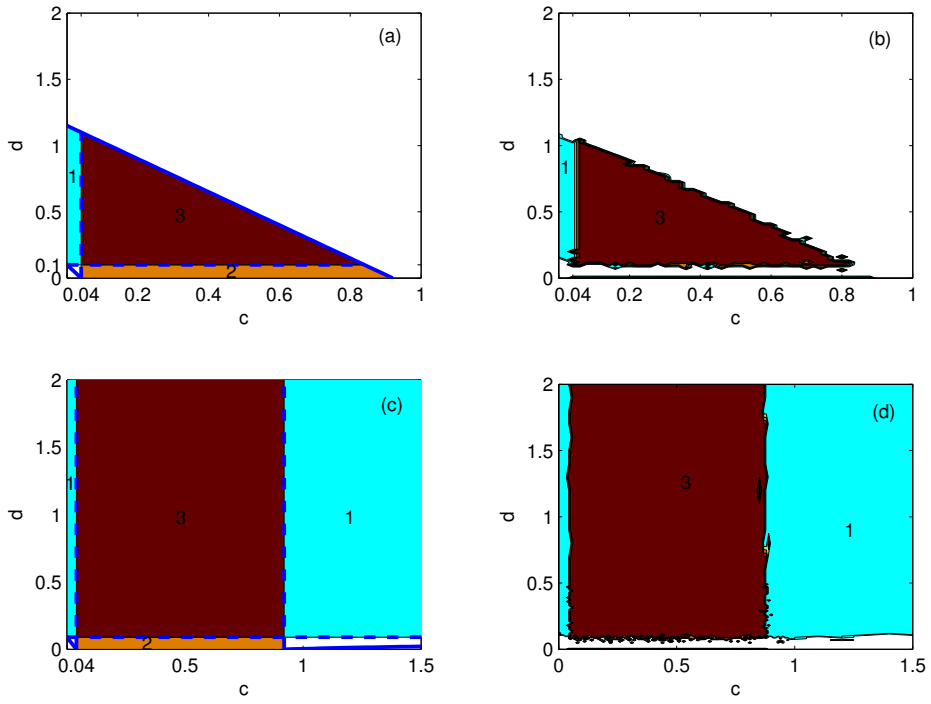

FIG. 12. The case of non-commutative supra-Laplacian matrices. Network synchronized regions from master stability equations (left) and numerical synchronization areas (right) for Rössler networks with identical fully-connected intra-layer topologies and nonidentical one-to-one coupling weights between layers. Here the inter-layer supra-Laplacian matrix $\mathcal{L}^I = [1\ -1; -1\ 1] \otimes \mathrm{diag}\{2,1,1,1,1\}$, $H = I_{11}$ and $\Gamma = I_{11}$ for (a)(b), and $H = I_{11}$ and $\Gamma = I_{22}$ for (c)(d).

layer, Eq. (5), allowing us to calculate the necessary region for intra-layer synchronization. In the limit of no intra-layer coupling the multiplex MSF reduces to a master stability equation for each independent inter-layer network, Eq. (6), allowing us to calculate the necessary region for inter-layer synchronization.

To explicitly use the multiplex MSF framework requires specifying $f(\cdot)$ (i.e., the internal nodal dynamics), and the inter- and intra-layer coupling functions (i.e., H and Γ respectively). We consider specifically a two-layer network of Rössler oscillators and various forms of H and Γ. We find that the different types of coherent behaviors observed in the network are determined by the intersections of the three necessary regions describing complete synchronization, intra-layer synchronization and inter-layer synchronization. Given a specified network topology, these regions can then be parameterized by the intra- and inter-layer coupling strengths (i.e., c and d respectively). Complete synchronization is stable when

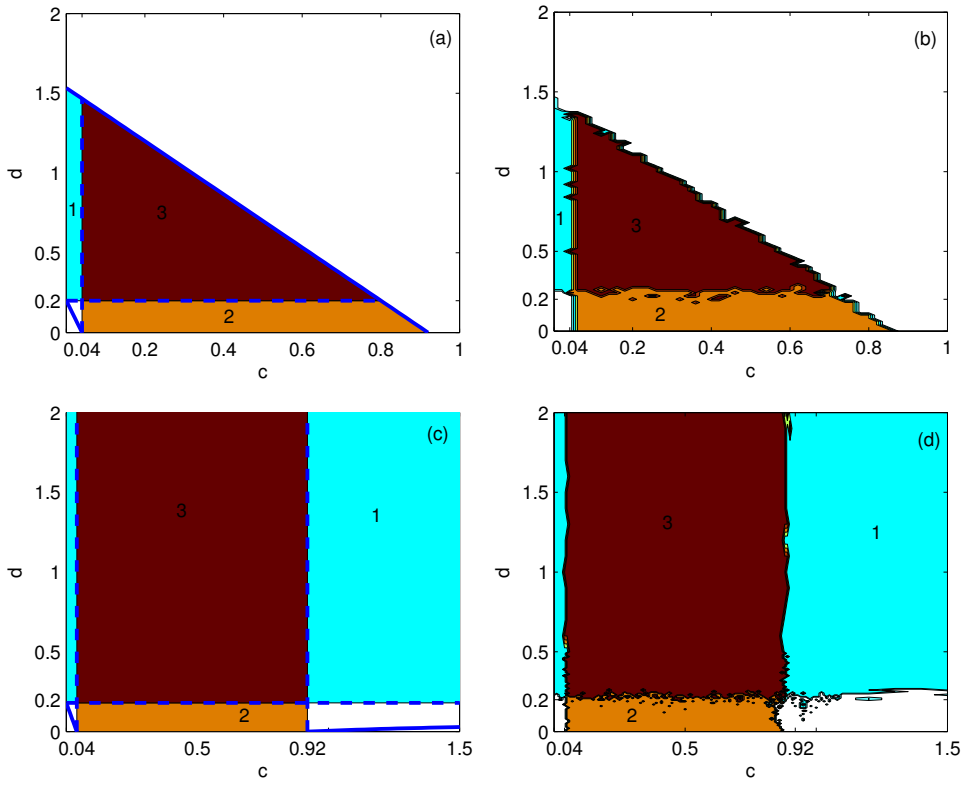

FIG. 13. The case of a three-layer fully-connected network, the inter-layer linking is a link (layer I —layer II—layer III) Network synchronized regions from master stability equations (left) and numerical synchronization areas (right) for Rössler networks with different combinations of H and Γ. (a)(c) $H = I_{11}$ and $\Gamma = I_{11}$, (b)(d) $H = I_{11}$ and $\Gamma = I_{22}$.

both c and d fall into the overlap of the three regions. Intra-layer synchronization is stable when both c and d fall into the overlap of the joint synchronized region and the intra-layer synchronized region. Inter-layer synchronization is stable when both c and d fall into the overlap of the joint synchronized region and the inter-layer synchronized region.

For a given network nodal dynamics, the joint synchronized region is mainly determined by both inner coupling matrices H and Γ. Similarly, the intra-layer synchronized region is mainly determined by the intra-layer coupling matrix H, and the inter-layer synchronized region by the inter-layer coupling matrix Γ. Therefore, in addition to nodal dynamics, the inner coupling function is an essential factor to determine which kind of synchronization the network will arrive at. If H is in such a form that the intra-layer synchronized region is empty, intra-layer synchronization is unstable regardless of however large the intra-layer coupling strength is. Similarly, if Γ is in such a form that the inter-layer synchronized region

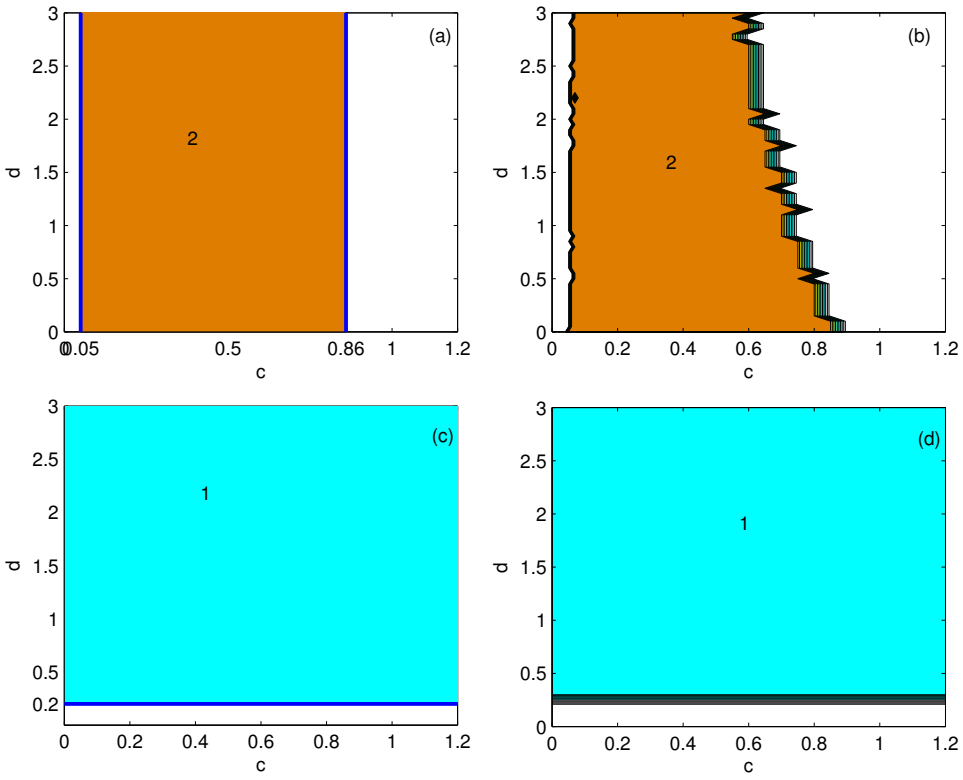

FIG. 14. The case of a three-layer fully-connected network, the inter-layer linking is a link (layer I —layer II—layer III) Network synchronized regions from master stability equations (left) and numerical synchronization areas (right) for Rössler networks with different combinations of H and Γ. (a)(c) $H = I_{11}$ and $\Gamma = I_{13}$, (b)(d) $H = I_{13}$ and $\Gamma = I_{22}$.

is empty, inter-layer synchronization is unstable regardless of however large the inter-layer coupling strength is. In either case, complete synchronization will not occur regardless of the coupling strength.

Here we have theoretically and numerically investigated specific duplex networks of Rössler oscillators where the two layers have the same topological structure. Our approach can be applied to multiplex networks with different choices for the internal nodal dynamics, different inter- and intra-layer coupling functions, and more layers.

As this work introduces a systematic approach for analyzing synchronization patterns in multiplex networks, the focus here is on the simplest case of multiplex networks where the supra-Laplacian matrix of the intra-layer connections is commutative with that of the inter-layer connections. Our framework further holds provided that the multiplex network has intra-layer topology that is identical on each layer and that both the intra-layer Lapla-

cian matrix L^L and the inter-layer Laplacian matrix L^I can be diagonalizable and have real eigenvalues. We verify numerically in section IV that the master stability equations derived herein can apply to a broader class of multiplex networks with non-commutative supra-Laplacians, but we can predict only the region of complete synchronization and intra-layer synchronization, or the region of complete synchronization and inter-layer synchronization, and we cannot simultaneously predict the overlap of these three synchronization behaviors. Establishing the exact minimal conditions under which our framework can be applied remains an important open question.

ACKNOWLEDGMENTS

This work is supported in part by the National Key Research and Development Program of China under Grant 2016YFB0800401, in part by the National Natural Science Foundation of China under Grants 61573004, 11501221, 61573262, 61621003 and 61532020, in part by the U.S. Army Research Office under Multidisciplinary University Research Initiative Award No. W911NF-13-1-0340 and Cooperative Agreement W911NF-09-2-0053, in part by the Program for New Century Excellent Talents in Fujian Province University in 2016 and in part by the Promotion Program for Young and Middle-aged Teacher in Science and Technology Research of Huaqiao University (ZQN-YX301).

Appendix A: Lyapunov Exponents

The Lyapunov Exponent measures the exponential contraction or expansion rate of infinitesimal perturbations. For n-dimensional continuous-time dynamical system

$$\dot{\boldsymbol{x}} = G(\boldsymbol{x}) \tag{A1}$$

Lyapunov Exponents are determined by the linearized equation with respect to the reference trajectory $\boldsymbol{s}(t)$

$$\dot{\boldsymbol{U}} = J(\boldsymbol{s(t)})\boldsymbol{U}$$

with initial condition $\boldsymbol{U}(0)$, where J is the Jacobian matrix of G, and $\boldsymbol{s}(t)$ satisfies Eq.(A1). Let $\boldsymbol{v}_i(0)(i = 1, 2, \cdots, n)$ is the orthonormal vector of $\boldsymbol{U}(0)$. The Lyapunov Exponents are

defined as follow

$$\sigma_i = \lim_{t\to\infty} \frac{1}{t} \ln ||\boldsymbol{U}(t)\boldsymbol{v}_i(0)||,$$

and the largest one is called the largest Lyapunov exponent (which is greater than zero for chaotic systems). It plays a key role in the stability analysis of controlled systems. One can adjust the parameter (here the coupling strength) such that the largest Lyapunov exponent is less than zero, and thus the system is controlled to the desire trajectory.

Appendix B: Decoupling the multiplex network system

Suppose that supra-Laplacian matrices $\mathcal{L}^L$ and $\mathcal{L}^I$ are symmetric matrices, and satisfy $\mathcal{L}^L\mathcal{L}^I = \mathcal{L}^I\mathcal{L}^L$, then there exists an invertible matrix P such that

$$P^{-1}\mathcal{L}^L P = \text{diag}\{\lambda_1, \cdots, \lambda_M, \lambda_{M+1}, \cdots, \lambda_{M\times N}\},$$

$$P^{-1}\mathcal{L}^I P = \text{diag}\{\mu_1, \cdots, \mu_M, \mu_{M+1}, \cdots, \mu_{M\times N}\},$$

where $0 = \lambda_1 = \cdots = \lambda_M < \lambda_{M+1} \leq \cdots \leq \lambda_{M\times N}$, $\mu_k \geq 0$ $(k = 1, 2, \cdots, M \times N)$, and $\text{diag}\{\upsilon_1, \cdots, \upsilon_M\}$ denotes a diagonal matrix whose j-th diagonal element is υ_j $(j = 1, 2, \cdots, M)$.

By denoting a new vector $\boldsymbol{\eta} = [\boldsymbol{\eta}_1^\top, \boldsymbol{\eta}_2^\top, \cdots, \boldsymbol{\eta}_{M\times N}^\top]^\top = (P \otimes I_m)^{-1}\boldsymbol{\xi}$, we can turn the variational equation (3) into

$$\dot{\boldsymbol{\eta}} = [I_{M\times N} \otimes Df(\boldsymbol{s}) - c(\text{diag}\{\lambda_1, \cdots, \lambda_{M\times N}\} \otimes H) - d(\text{diag}\{\mu_1, \cdots, \mu_{M\times N}\} \otimes \Gamma)]\boldsymbol{\eta}. \quad \text{(B1)}$$

It further yields

$$\dot{\boldsymbol{\eta}}_k = [Df(\boldsymbol{s}) - c\lambda_k H - d\mu_k \Gamma]\boldsymbol{\eta}_k, \quad k = 1, 2, \cdots, M \times N. \quad \text{(B2)}$$

Here, $\boldsymbol{\eta}_k$ represents the mode of perturbation in the generalized eigenspace associated with λ_k and μ_k. A criterion for the synchronization manifold to be (asymptotically) stable is that all the transversal Lyapunov exponents of the variational equation (B2) are strictly negative. Clearly, these Lyapunov exponents depend on the node dynamics $f(\cdot)$, the network intra- and inter-layer coupling strengths c and d, and the coupling matrices H and Γ. Consequently, we can get the three master stability equations: Eqs. (4), (5) and (6).

Appendix C: Calculating synchronized regions $\mathbf{R_{c,d}}$

We can calculate three synchronized regions with regard to parameters α and β: R, R^{Intra} and R^{Inter} from Eqs. (4), (5) and (6), respectively. Furthermore, when the network topologies are given, we can directly calculate the characteristic values of supra-Laplacian matrices and parameterize those regions in terms of c and d, since $\alpha = c\lambda$ and $\beta = d\mu$.

For example, when $H = I_{11}$ and $\Gamma = I_{11}$, the nonzero characteristic modes $\alpha = c\lambda$ and $\beta = c\mu$ should lie in $R_{\alpha,\beta} = \{(\alpha, \beta)|\, 0.2 < \alpha + \beta < 4.6\}$, and consequently the region with respect to parameters c and d is

$$R_{c,d} = \{(c, d)|\, 0.2 < c + 2d, c + 0.4d < 0.92\}.$$

For other combinations of H and Γ, the synchronized regions with respect to parameters c and d can be similarly obtained.

Appendix D: Synchronization errors & Indicator function.

To measure the extent of intra-layer, inter-layer and complete synchronization, we introduce the following indices:

$$E^{(k)}_{Intra}(t) = \frac{1}{N}\sum_{i=1}^{N} \|x_i^{(k)}(t) - \overline{x}^{(k)}(t)\|,\ k = 1, 2, \cdots, M \tag{D1}$$

where $\|\cdot\|$ is a norm operator, and $\overline{x}^{(k)}(t)$ is the average state of all the nodes in the kth layer at time t. Thus $E^{(k)}_{Intra}(t)$ is the synchronization error of nodes in the kth layer at time t, namely, the intra-layer synchronization error.

Similarly, the inter-layer synchronization error is defined as

$$E_{Inter}(t) = \frac{1}{MN}\sum_{i=1}^{N}\sum_{k=1}^{M} \|x_i^{(k)}(t) - \overline{x}_i(t)\|, \tag{D2}$$

and the complete synchronization error is defined as

$$E(t) = \frac{1}{NM}\sum_{k=1}^{M}\sum_{i=1}^{N} \|x_i^{(k)}(t) - \overline{x}(t)\|, \tag{D3}$$

where $\overline{x}_i(t)$ is the average state of the node i in each layer and its counterparts in other layers, and $\overline{x}(t)$ is that of all the nodes in the multiplex network.

With these definitions, we use the following indicator function to represent complete synchronization, intra-layer synchronization and inter-layer synchronization:

$$I_d = \begin{cases} 3,\ E_{Inter}(t) < \epsilon \text{ and } E^{(k)}_{Intra}(t) < \epsilon \text{ for all } t > T_0, \\ 2,\ E_{Inter}(t) \geq \epsilon \text{ and } E^{(k)}_{Intra}(t) < \epsilon \text{ for all } t > T_0, \\ 1,\ E_{Inter}(t) < \epsilon \text{ and } E^{(k)}_{Intra}(t) \geq \epsilon \text{ for all } t > T_0, \\ 0,\ \text{other.} \end{cases} \tag{D4}$$

Here, T_0 is a time threshold value and ϵ is a given threshold for synchronization errors. In the simulations, $\epsilon = 1.0 \times 10^{-2}$, and $T_0 = 0.8T_{total}$ (T_{total} is the total evolution time). It is obvious that the network reaches complete synchronization when $I_d = 3$, intra-layer synchronization when $I_d = 2$, inter-layer synchronization when $I_d = 1$, and none of the above when $I_d = 0$.

Appendix E: Theoretical analysis for the case of complete synchronization

Consider a duplex network composed of two subnetworks with the same internal topology and one-to-one inter-layer connectivity between nodes. The dynamical evolution can be written as:

$$\begin{cases} \dot{\boldsymbol{x}}_i = f(\boldsymbol{x}_i) - c\sum_{j=1}^{N} l_{ij} H \boldsymbol{x}_j - d\,\Gamma(a\boldsymbol{x}_i - a\boldsymbol{y}_i), \\ \dot{\boldsymbol{y}}_i = f(\boldsymbol{y}_i) - c\sum_{j=1}^{N} l_{ij} H \boldsymbol{y}_j - d\,\Gamma(b\boldsymbol{y}_i - b\boldsymbol{x}_i), \end{cases} \quad i = 1, 2, \cdots, N. \tag{E1}$$

Here the inter-layer Laplacian matrix $L^I = \begin{pmatrix} a & -a \\ -b & b \end{pmatrix}$ (a and b are nonnegative real constants satisfying $a^2 + b^2 \neq 0$), indicating that the information exchange between layers is asymmetric and weighted when $a \neq b$. Note, the duplex network (E1) with $a = b = 1$ has been discussed in the main text. The intra-layer and inter-layer supra-Laplacian matrices, $\mathcal{L}^L = I_2 \otimes L$ and $\mathcal{L}^I = L^I \otimes I_N$ satisfy the commutative condition, where $L = (l_{ij})_{N\times N}$ is the intra-layer Laplacian matrix and I_m is an identity matrix of order m.

Next, we will theoretically explain how the observed synchronization patterns require the overlap of the different regions of synchronization from two aspects: the intra-layer synchronization stability equations derived next in Sec. E 1 and the inter-layer synchronization stability equations derived in Sec. E 2.

1. Intra-layer synchronization stability equations

Let $\boldsymbol{s}_x(t)$ and $\boldsymbol{s}_y(t)$ denote the intra-layer synchronous states of the x-layer and y-layer, respectively, which are dominated by the following equations:

$$\begin{cases} \dot{\boldsymbol{s}_x} = f(\boldsymbol{s}_x) - ad\,\Gamma(\boldsymbol{s}_x - \boldsymbol{s}_y), \\ \dot{\boldsymbol{s}_y} = f(\boldsymbol{s}_y) - bd\,\Gamma(\boldsymbol{s}_y - \boldsymbol{s}_x). \end{cases} \tag{E2}$$

Linearizing the duplex network (E1) at the intra-layer synchronous states $\boldsymbol{s}_x$ and $\boldsymbol{s}_y$ yields

$$\begin{cases} \delta\dot{\boldsymbol{x}}_i = Df(\boldsymbol{s}_x)\delta\boldsymbol{x}_i - ad\,\Gamma(\delta\boldsymbol{x}_i - \delta\boldsymbol{y}_i) - c\sum\limits_{j=1}^{N} l_{ij}H\delta\boldsymbol{x}_j, \\ \delta\dot{\boldsymbol{y}}_i = Df(\boldsymbol{s}_y)\delta\boldsymbol{y}_i - bd\,\Gamma(\delta\boldsymbol{y}_i - \delta\boldsymbol{x}_i) - c\sum\limits_{j=1}^{N} l_{ij}H\delta\boldsymbol{y}_j, \end{cases} \quad i = 1, 2, \cdots, N. \tag{E3}$$

Denote $\delta\boldsymbol{z}_i = (\delta\boldsymbol{x}_i^T,\, \delta\boldsymbol{y}_i^T)^T$, $\widetilde{Df}(\boldsymbol{s}_x, \boldsymbol{s}_y) = \begin{pmatrix} Df(\boldsymbol{s}_x) & 0 \\ 0 & Df(\boldsymbol{s}_y) \end{pmatrix}$, $\delta\boldsymbol{z} = (\delta\boldsymbol{z}_1^T, \delta\boldsymbol{z}_2^T, \cdots, \delta\boldsymbol{z}_N^T)^T$, then Eq. (E3) can be rewritten as

$$\delta\dot{\boldsymbol{z}} = I_N \otimes [\widetilde{Df}(\boldsymbol{s}_x, \boldsymbol{s}_y) - d\,(L^I \otimes \Gamma)]\delta\boldsymbol{z} - c(L \otimes (I_2 \otimes H))\delta\boldsymbol{z}. \tag{E4}$$

Since the Laplacian matrix $L = (l_{ij})$ is symmetric (assuming links within each layer are undirected), there exists an invertible matrix P such that

$$P^{-1}LP = \begin{pmatrix} \lambda_1 & & & \\ & \lambda_2 & & \\ & & \ddots & \\ & & & \lambda_N \end{pmatrix},$$

here $0 = \lambda_1 < \lambda_2 \leq \lambda_3 \leq \cdots \leq \lambda_N$. Letting $\boldsymbol{\xi} = (P \otimes I_{2m})^{-1}\delta\boldsymbol{z}$, and $\boldsymbol{\xi} = (\boldsymbol{\xi}_1^T, \boldsymbol{\xi}_2^T, \cdots, \boldsymbol{\xi}_N^T)^T$, we have

$$\dot{\boldsymbol{\xi}}_j = [\widetilde{Df}(\boldsymbol{s}_x, \boldsymbol{s}_y) - d\,(L^I \otimes \Gamma)]\boldsymbol{\xi}_j - c\lambda_k(I_2 \otimes H)\boldsymbol{\xi}_j, \quad j = 1, 2, \cdots, N.$$

Neglecting the subscript j, we can obtain the general form of the master stability equation for intra-layer synchronization:

$$\dot{\boldsymbol{\eta}} = [\widetilde{Df}(\boldsymbol{s}_x, \boldsymbol{s}_y) - d\,(L^I \otimes \Gamma)]\boldsymbol{\eta} - \alpha(I_2 \otimes H)\boldsymbol{\eta}, \tag{E5}$$

where $\alpha = c\lambda$, and λ is any non-zero eigenvalue of Laplacian matrix L.

If the duplex network (E1) reaches complete synchronization, it means that the two intra-layer synchronous states $\boldsymbol{s}_x$ and $\boldsymbol{s}_y$ converge to the same state $\boldsymbol{s}$ dominated by the isolated nodal system: $\dot{\boldsymbol{s}} = f(\boldsymbol{s})$. Then the variational equation of (E2) at $\boldsymbol{s}$

$$\dot{\delta\boldsymbol{s}} = [Df(\boldsymbol{s}) - (a+b)d\Gamma]\delta\boldsymbol{s}$$

should be stable. Since the eigenvalues of $L^I = \begin{pmatrix} a & -a \\ -b & b \end{pmatrix}$ are $\mu = 0, a+b$, and $\beta = \mu d$ where μ is the nonzero eigenvalue, the above variational equation can be accordingly transformed into the general form as follow:

$$\dot{\delta\boldsymbol{s}} = [Df(\boldsymbol{s}) - \beta\Gamma]\delta\boldsymbol{s}, \tag{E6}$$

which is stable for $\beta \in R_\beta^{Inter}$ and any value of coupling strength α. This yields

$$R_\beta^{Inter} = \{\beta \,|\sigma(\beta) < 0\},$$

where $\sigma(\beta)$ is the largest Lyapunov exponent of equation (E6). For convenience, we include the parameter α into R_β^{Inter}, and obtain

$$R_{\alpha,\beta}^{Inter} = \{(\alpha,\beta) \,|\sigma(\beta) < 0, \alpha \geq 0\}. \tag{E7}$$

We call $R_{\alpha,\beta}^{Inter}$ the inter-layer synchronized region with respect to α and β.

Simultaneously, when the duplex network arrives at complete synchronization, Eq. (E5) is stable at $\boldsymbol{s}$, meaning that the following equation is stable at the origin:

$$\dot{\boldsymbol{\eta}} = [I_2 \otimes Df(\boldsymbol{s}) - d\,(L^I \otimes \Gamma)]\boldsymbol{\eta} - \alpha(I_2 \otimes H)\boldsymbol{\eta}. \tag{E8}$$

Diagonalizing the matrix $L^I = \begin{pmatrix} a & -a \\ -b & b \end{pmatrix}$, and making a simple linear transformation, we can get the decoupled equations from (E4):

$$\dot{\boldsymbol{\zeta}}_1 = [Df(\boldsymbol{s}) - \alpha H]\boldsymbol{\zeta}_1, \tag{E9}$$

and

$$\dot{\boldsymbol{\zeta}}_2 = [Df(\boldsymbol{s}) - \alpha H - (a+b)d\Gamma]\boldsymbol{\zeta}_2.$$

Similar to the argument above, replace $(a+b)d$ with β, and the second of the decoupled equations turns into

$$\dot{\boldsymbol{\zeta}}_2 = [Df(\boldsymbol{s}) - \alpha H - \beta\Gamma]\boldsymbol{\zeta}_2. \tag{E10}$$

Equation (E9) is stable when $\alpha \in R_{\alpha,\beta}^{Intra} \triangleq \{\alpha \,|\sigma(\alpha) < 0, \beta \geq 0\}$, here $\sigma(\alpha)$ is the largest Lyapunov exponent of Eq. (E9) with parameter α. Similarly, Eq.(E10) is stable when $(\alpha, \beta) \in R_{\alpha,\beta} \triangleq \{(\alpha, \beta) \,|\sigma(\alpha, \beta) < 0\}$, where $\sigma(\alpha, \beta)$ is the largest Lyapunov exponent of Eq. (E10). For convenience, we call $R_{\alpha,\beta}^{Intra}$, $R_{\alpha,\beta}^{Inter}$ and $R_{\alpha,\beta}$ the intra-layer, inter-layer and joint synchronized regions, respectively. Given a specified intra-layer network topology, $R_{\alpha,\beta}^{Intra}$, $R_{\alpha,\beta}^{Inter}$ and $R_{\alpha,\beta}$ can be parameterized by c (the intra-layer coupling strength) and d (the inter-layer coupling strength), denoted by $R_{c,d}^{Intra}$, $R_{c,d}^{Inter}$ and $R_{c,d}$, respectively.

In summary, to reach complete synchronization in the duplex network (E1), it is necessary that three synchronization stability equations, (E6), (E9) and (E10), are simultaneously stable. Thus, the intra-layer characteristic modes $\alpha = \lambda c$ and the inter-layer characteristic modes $\beta = \mu d$ have to fall into the the overlap of $R_{\alpha,\beta}^{Intra}$, $R_{\alpha,\beta}^{Inter}$ and $R_{\alpha,\beta}$, i.e. $R_{\alpha,\beta}^{Intra} \cap R_{\alpha,\beta}^{Inter} \cap R_{\alpha,\beta}$. It indicates that the intra-layer and inter-layer coupling strengths have to fall into the overlap of $R_{c,d}^{Intra}$, $R_{c,d}^{Inter}$ and $R_{c,d}$, i.e., $R_{c,d}^{Intra} \cap R_{c,d}^{Inter} \cap R_{c,d}$, when the intra-layer network topology L and the inter-layer linking way L^I are specified.

2. Inter-layer synchronization stability equations

In Sec. E 1 we started from the intra-layer synchronization stability equations, we can also analyze this problem from the inter-layer synchronization approach. Denote $\boldsymbol{s}_i(t)(i = 1, 2, \cdots, N)$ as the inter-layer synchronous states, which are dominated by the following equations:

$$\dot{\boldsymbol{s}}_i = f(\boldsymbol{s}_i) - c\sum_{j=1}^{N} l_{ij} H \boldsymbol{s}_j, \quad i = 1, 2, \cdots, N \tag{E11}$$

Linearize the duplex network (E1) at inter-layer synchronous states $\boldsymbol{s}_i$, then we obtain

$$\begin{cases} \delta\dot{\boldsymbol{x}}_i = Df(\boldsymbol{s_i})\delta\boldsymbol{x}_i - c\sum\limits_{j=1}^{N} l_{ij} H \delta\boldsymbol{x}_j - ad\,\Gamma(\delta\boldsymbol{x}_i - \delta\boldsymbol{y}_i), \\ \delta\dot{\boldsymbol{y}}_i = Df(\boldsymbol{s_i})\delta\boldsymbol{y}_i - c\sum\limits_{j=1}^{N} l_{ij} H \delta\boldsymbol{y}_j - bd\,\Gamma(\delta\boldsymbol{y}_i - \delta\boldsymbol{x}_i), \end{cases} \quad i = 1, 2, \cdots, N. \tag{E12}$$

Denoting $\delta\boldsymbol{z}_i = \delta\boldsymbol{x}_i - \delta\boldsymbol{y}_i$, we get from Eq.(E12) that

$$\delta\dot{\boldsymbol{z}}_i = Df(\boldsymbol{s}_i)\delta\boldsymbol{z}_i - c\sum_{j=1}^{N} l_{ij} H \delta\boldsymbol{z}_j - (a+b)d\,\Gamma\delta\boldsymbol{z}_i, \quad i = 1, 2, \cdots, N$$

Let $\delta \boldsymbol{Z} = (\delta \boldsymbol{z}_1^T, \delta \boldsymbol{z}_2^T, \cdots, \delta \boldsymbol{z}_N^T)^T$, we thus obtain the following master stability equation for inter-layer synchronization:

$$\delta \dot{\boldsymbol{Z}} = DF(\boldsymbol{s}_1, \boldsymbol{s}_2, \cdots, \boldsymbol{s}_N)\delta \boldsymbol{Z} - c(L \otimes H)\delta \boldsymbol{Z} - (a+b)d(I_N \otimes \Gamma)\delta \boldsymbol{Z}, \tag{E13}$$

where

$$DF(\boldsymbol{s}_1, \boldsymbol{s}_2, \cdots, \boldsymbol{s}_N) = \begin{pmatrix} Df(\boldsymbol{s}_1) & & & \\ & Df(\boldsymbol{s}_2) & & \\ & & \ddots & \\ & & & Df(\boldsymbol{s}_N) \end{pmatrix}.$$

It is worth noting that Eq.(E11) dominating the inter-layer synchronous state $\boldsymbol{s}_i(t)$ can be linearized at $\boldsymbol{s}(t)$ as

$$\delta \dot{\boldsymbol{s}}_i = Df(\boldsymbol{s})\delta \boldsymbol{s}_i - c\sum_{j=1}^{N} l_{ij} H \delta \boldsymbol{s}_j, \quad i = 1, 2, \cdots, N \tag{E14}$$

and can thus be rewritten as

$$\delta \dot{\boldsymbol{S}} = [I_N \otimes Df(\boldsymbol{s}) - c(L \otimes H)]\delta \boldsymbol{S}, \tag{E15}$$

where $\delta \boldsymbol{S} = (\delta \boldsymbol{s}^T, \delta \boldsymbol{s}^T, \cdots, \delta \boldsymbol{s}^T)^T$. Diagonalize the Laplacian matrix $L = (l_{ij})$, and we can get the decoupled equations

$$\dot{\boldsymbol{\xi}}_k = [Df(\boldsymbol{s}) - c\lambda_k H]\boldsymbol{\xi}_k, \quad k = 2, 3, \cdots, N, \tag{E16}$$

where $0 = \lambda_1 < \lambda_2 \leq \lambda_3 \leq \lambda_N$ are the eigenvalues of L, and the general form of (E16) is

$$\dot{\boldsymbol{\eta}} = [Df(\boldsymbol{s}) - \alpha H]\boldsymbol{\eta}. \tag{E17}$$

Now, if the duplex network (E1) achieves complete synchronization, which means that $\boldsymbol{s}_i (i = 1, 2, \cdots, N)$ converges to a synchronous state $\boldsymbol{s}$. It is thus necessary to require that Eq. (E17) is stable. Obviously, Eq. (E17) is stable at origin when $\alpha \in R_{\alpha,\beta}^{Intra} \triangleq \{\alpha \,|\sigma(\alpha) < 0, \beta \geq 0\}$ ($\sigma(\alpha)$ is the largest Lyapunov exponent of Eq. (E17)). Given the intra-layer structure and inter-layer linking way, $R_{\alpha,\beta}^{Intra}$ can be parameterized by the coupling strengths c and d, denoted by $R_{c,d}^{Intra}$.

Simultaneously, let $\boldsymbol{s}$ substitute $\boldsymbol{s}_i (i = 1, 2, \cdots, N)$ in Eq. (E13), there is

$$\delta \dot{\boldsymbol{Z}} = [I_N \otimes Df(\boldsymbol{s}) - c(L \otimes H)]\delta \boldsymbol{Z} - (a+b)d(I_N \otimes \Gamma)\delta \boldsymbol{Z}. \tag{E18}$$

Diagonalizing the matrix L, and performing a simple linear transformation, one can get the following decoupled equations:

$$\dot{\boldsymbol{\zeta}}_1 = [Df(\boldsymbol{s}) - (a+b)d\Gamma]\boldsymbol{\zeta}_1,$$

$$\dot{\boldsymbol{\zeta}}_2 = [Df(\boldsymbol{s}) - \alpha H - (a+b)d\Gamma]\boldsymbol{\zeta}_2.$$

Similar to the handling way in (I), replace $(a+b)d$ with β, the above decoupled equations can be turned into

$$\dot{\boldsymbol{\zeta}}_1 = [Df(\boldsymbol{s}) - \beta\Gamma]\boldsymbol{\zeta}_1, \tag{E19}$$

$$\dot{\boldsymbol{\zeta}}_2 = [Df(\boldsymbol{s}) - \alpha H - \beta\Gamma]\boldsymbol{\zeta}_2. \tag{E20}$$

Equation (E19) is stable when $\beta \in R_{\alpha,\beta}^{Inter} \triangleq \{\beta \,|\sigma(\beta) < 0, \alpha \geq 0\}$, here $\sigma(\beta)$ is the largest Lyapunov exponent of Eq. (E19). Similarly, Eq. (E20) is stable when $(\alpha,\beta) \in R_{\alpha,\beta} \triangleq \{(\alpha,\beta)\,|\sigma(\alpha,\beta) < 0\}$, and $\sigma(\alpha,\beta)$ is the largest Lyapunov exponent of Eq. (E20). For convenience, we call $R_{\alpha,\beta}^{Intra}$, $R_{\alpha,\beta}^{Inter}$ and $R_{\alpha,\beta}$ the intra-layer, inter-layer and joint synchronized regions, respectively. Given a specified intra-layer network topology, $R_{\alpha,\beta}^{Intra}$, $R_{\alpha,\beta}^{Inter}$ and $R_{\alpha,\beta}$ can be parameterized by c (the intra-layer coupling strength) and d (the inter-layer coupling strength), denoted by $R_{c,d}^{Intra}$, $R_{c,d}^{Inter}$ and $R_{c,d}$, respectively.

In summary, to obtain complete synchronization in duplex network (E1), it is necessary that Eqs. (E17), (E19) and (E20) are simultaneously stable. This works when $(\alpha,\beta) \in R_{\alpha,\beta}^{Intra} \cap R_{\alpha,\beta}^{Inter} \cap R_{\alpha,\beta}$, or when $(c,d) \in R_{c,d}^{Intra} \cap R_{c,d}^{Inter} \cap R_{c,d}$ after the intra-layer topology and inter-layer linking way are definitely given. It again verifies that complete synchronization occurs in the overlap of $R_{\alpha,\beta}^{Intra}$, $R_{\alpha,\beta}^{Inter}$ and $R_{\alpha,\beta}$.

Appendix F: A real-world example, the CORS system

The network of Continuously Operating Reference Stations (CORS) [39] system consists of continuously operating Global Navigation Satellite System (GNSS) reference stations, a communication network and data centers. Through continuous observation by GNSS satellites and GNSS measurement processing, the CORS system is widely applied to various fields such as: three dimensional positioning, navigation and timing at different accuracy levels, satellite orbit tracking and determination, maintaining the reference framework of the earth, geodynamics research such as earthquake and plate movements, and sea level, ionospheric

and water vapor monitoring. The CORS system is an essential geospatial information infrastructure with many countries and regions of the world, such as China, America, Europe and Australia having established CORS systems.

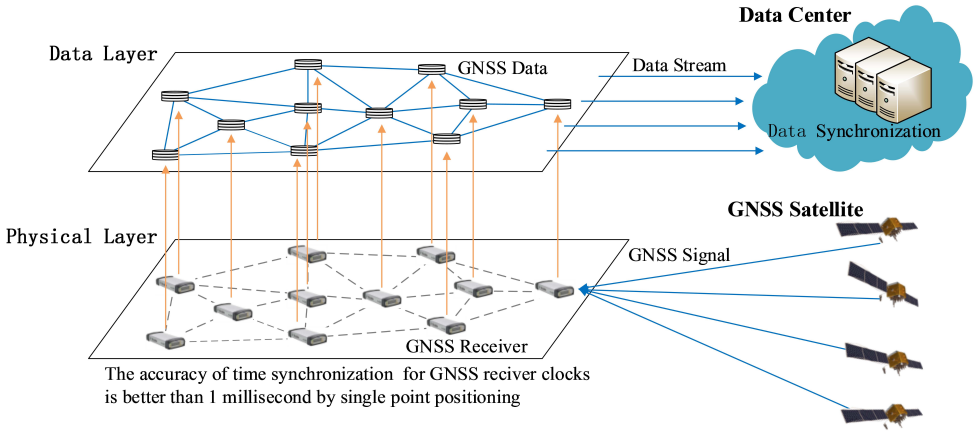

FIG. 15. A diagram of CORS systems in China's BeiDou Navigation Satellite System. The below layer is the physical layer composed of some GNSS receivers, and the top layer is the corresponding data-processing layer.

The CORS system can be regarded as a multi-layer network composed of a physical layer and a data layer, as shown in Fig. 15. The physical layer consists of N receivers, tracking the same m satellites, to receive the positioning data. Because there exist biased clocks between receivers, these receivers have to adjust their clocks and obtain time synchronization to improve the precision of positioning [41, 42]. That is to say, intra-layer synchronization with respect to time is required in the physical layer. However, the processing of the data is not done by the receivers, but instead by data processing units in Data Centers [40]. These data processing units respectively link their receivers forming a virtual data layer (top layer in Fig. 15), and a Synchronous Digital Hierarchy (SDH) Network. Each unit in the Data Layer needs to achieve data synchronization for accurate positioning, implying that the Data layer needs to achieve intra-layer synchronization.

[1] D. J. Watts and S. H. Strogatz, Nature **393**, 440 (1998).

[2] M. Barahona and L. M. Pecora, Phys. Rev. Lett. **89**, 054101 (2002).

[3] H. Hong, M. Y. Choi, and B. J. Kim, Phys. Rev. E **65**, 026139 (2002).

[4] M. E. J. Newman, SIAM Rev. **45**, 167 (2003).

[5] J. Lü, X. Yu, G. Chen, and D. Cheng, IEEE Trans. Circuits Syst. I **51**, 787 (2004).

[6] J. Lü and G. Chen, IEEE Trans. Automat. Contr. **50**, 841 (2005).

[7] J. Zhou, J. A. Lu, and J. Lü, IEEE Trans. Automat. Contr. **51**, 652 (2006).

[8] C. W. Wu, Synchronization in Complex Network of Nonlinear Dynamical System (World Scientific, Singapore, 2007) pp. 51–123.

[9] S. Boccalettia, V. Latorab, Y. Morenod, M. Chavezf, and D.-U. Hwang, Phys. Rep. **424**, 175 (2006).

[10] A. Arenas, A. Díaz-Guilera, J. Kurths, Y. Morenob, and C. Zhou, Phys. Rep. **469**, 93 (2008).

[11] Y. Chen, J. Lü, F. Han, and X. Yu, Syst. Contr. Lett. **60**, 517 (2011).

[12] L. Huang, Y. C. Lai, and R. A. Gatenby, Chaos **18**, 013101 (2008).

[13] L. Donetti, P. I. Hurtado, and M. A. Muńoz, Phys. Rev. Lett. **95**, 188701 (2005).

[14] L. M. Pecora, F. Sorrentino, A. M. Hagerstrom, T. E. Murphy, and R. Roy, Nat. Commun. **5**, 4079 (2014).

[15] L. Tang, J. A. Lu, and G. Chen, Chaos **22**, 023121 (2012).

[16] C. D. Brummitt, R. M. D'Souza, and E. A. Leicht, Proc. Natl Acad. Sci. U.S.A. **109**, E680 (2012).

[17] F. Radicchi and A. Arenas, Nat. Phys. **9**, 717 (2013).

[18] S. Gómez, A. Díaz-Guilera, J. G.-G. nes, C. J. Pérez-Vicente, Y. Moreno, and A. Arenas, Phys. Rev. Lett. **110**, 028701 (2013).

[19] M. D. Domenico, A. Solé-Ribalta, S. Gómez, and A. Arenas, Proc. Natl. Acad. Sci. U.S.A. **111**, 8351 (2014).

[20] G. D'Agostino and A. Scala, Networks of Networks: the last Frontier of Complexity (Springer, Berlin, 2014).

[21] T. Valles-Catala, F. A. Massucci, R. Guimera, and M. Sales-Pardo, Phys. Rev. X **6**, 011036 (2016).

[22] M. Kivelä, A. Arenas, M. Barthelemy, J. P. Gleeson, Y. Moreno, and M. A. Porter, J. Complex Netw. **2**, 203 (2014).

[23] S. Boccaletti, G. Bianconi, R. Criado, C. D. Genio, J. Gómez-Gardeñes, M. Romance, I. Sendiña-Nadal, Z. Wang, and M. Zanin, Phys. Rep. **544**, 1 (2014).

[24] O. Yagan, D. Qian, J. Zhang, and D. Cochran, IEEE Journal on Selected Areas in Commu-

nications **31**, 1038 (2013).

[25] L. M. Pecora and T. L. Carroll, Phys. Rev. Lett. **80**, 2109 (1998).

[26] L. Tang, J. A. Lu, J. Lü, and X. Yu, Int. J. Bifurcat. Chaos **22**, 1250282 (2012).

[27] L. Tang, J. A. Lu, J. Lü, and X. Wu, Int. J. Bifurcat. Chaos **24**, 1450011 (2014).

[28] L. Tang, X. Wu, J. Lü, and J. A. Lu, Chaos **25**, 033101 (2012).

[29] A. Solé-Ribalta, M. D. Domenico, N. E. Kouvaris, A. Díaz-Guilera, S. Gómez, and A. Arenas, Phys. Rev. E **88**, 032807 (2013).

[30] J. Aguirre, R. Sevilla-Escoboza, R. Gutiérrez, D. Papo, and J. M. Buldú, Phys. Rev. Lett. **112**, 248701 (2014).

[31] M. Xu, J. Zhou, J. A. Lu, and X. Wu, Eur. Phys. J. B **88**, 240 (2015).

[32] Y. Li, X. Wu, J. A. Lu, and J. Lü, IEEE Trans. Circuits Sys. II: Express Briefs **63**, 206 (2015).

[33] F. Sorrentino, New J. Phys. **14**, 033035 (2012).

[34] D. Irving and F. Sorrentino, Phys. Rev. E **86**, 056102 (2012).

[35] C. I. D. Genio, J. Gómez-Gardeñes, I. Bonamassa, and S. Boccaletti, Science Advances **2**, no. 11 (2016).

[36] L. V. Gambuzza, M. Frasca, and J. G.-G. nes, EPL **110**, 20010 (2015).

[37] R. Sevilla-Escoboza, I. S. na Nadal, I. Leyva, R. Gutiérrez, J. M. Buldú, and S. Boccaletti, Chaos **26**, 065304 (2016).

[38] G. A. Leonov and N. V. Kuznetsov, Int. J. Bifurcat. Chaos **17**, 1079 (2007).

[39] C. Rizos, GPS Solut. **11**, 151 (2007).

[40] G. Blewitt, in GPS for Geodesy, edited by P. Teunissen and A. Kleusberg (Springer, Berlin Heidelberg, 1998) pp. 231–270.

[41] H. Liu, R. F. Zhang, J. N. Liu, and M. Zhang, Sci. China Tech. Sci. **59**, 9 (2016).

[42] D. Kim and R. B. Langley, Navigation-Alexandria **49**, 205 (2002).